Universitetet i Stavanger

FACULTY OF SCIENCE AND TECHNOLOGY

MASTER'S THESIS

Study programme/specialisation: Biological chemistry	Spring / Autumn semester, 2018 Open
Author: Phuong Tuyet Nguyen	…… (signature of author)
Programme coordinator: Kåre Bredeli Jørgensen Supervisor(s): Grete Jonsson	
Title of master's thesis: Detection of Nrf2 in peripheral blood mononuclear cells: comparison and application of two methods	
Credits: 60	
Keywords: Nuclear factor erythroid 2-related factor 2 (Nrf2), oxidative stress, biomarkers, peripheral blood mononuclear cells (PBMCs), Western blot, ELISA-based kit	Number of pages: 65 + supplemental material/other: 7 Stavanger, 01.11.2018

Title page for Master's Thesis
Faculty of Science and Technology

Acknowledgements

I would like to express my very great appreciation and sincere thanks to my external supervisor, Grete Jonsson. Her valuable and constructive advice and suggestions guided me in the right direction. Her office door was always open whenever I had questions about my research.

I convey my grateful thanks to my faculty supervisor, Kåre Bredeli Jørgensen, for his useful and insightful comments and recommendations and to Professor Roald Omdal for giving me the opportunity to do the research at Stavanger University Hospital.

My deepest gratitude is also extended to Kjetil Bårdsen for his patient and comprehensive guidance and always be supportive when I needed assistance. His willingness and generosity to share his immense knowledge and take the time to help me throughout the research process have been very strongly appreciated.

I would also like to take this opportunity to express my sincere thanks to Live Egeland Eidem and Ingeborg Kvivik for the welcoming work environment they created and the brilliant comments they gave me.

Special thanks to my colleagues at Department of Medical Biochemistry for samples and to Lene Mikkelsen and the staff of Hematology section for help in cell count. Many thanks to David Cox, Jhen Cox, and Ben Cochrane for advice on writing. Thanks to my friends for their understanding and support.

Finally, I wish to thank my family, especially my mother Tuyet and my brother Sang for their encouragement, understanding and love.

Abstract

Protein nuclear factor erythroid 2-related factor 2 (Nrf2) is a transcription factor that regulates expression of numerous proteins. These proteins protect cells against oxidative stress and reinstate cellular homeostasis. Oxidative stress activates Nrf2, leading to its translocation and accumulation in the nucleus.

Oxidative stress is defined as an imbalance between the production of reactive oxygen species (ROS) and the cellular antioxidant defense capacity, in favor of the ROS. Oxidative stress has been associated with ageing and diseases including cancer, diabetes, atherosclerosis, inflammation, and neurodegeneration.

Since Nrf2 is ubiquitously expressed in all tissues, and Nrf2 levels and cellular location change during oxidative stress, it is desirable to establish a method to evaluate the state of Nrf2 in both cytoplasm and nuclear fractions. Peripheral blood mononuclear cells (PBMCs) can be obtained in a non-invasive manner by blood sampling and are therefore a preferable model system for monitoring Nrf2 levels and localization in response to oxidative stress. At Stavanger University Hospital, biomarkers such as protein carbonyls (PC), malondialdehyde (MDA), and advanced oxidation protein products (AOPP) in blood samples from patients have been used in different studies to assess oxidative stress induced by diseases. Nrf2 determination, if successful, can then become a supplementary test in addition to the tests of the aforementioned conventional biomarkers.

In this research, Western blot and an enzyme-linked immunosorbent assay (ELISA)-based TransAM Nrf2 kit were utilized for the detection of Nrf2 in PBMCs. Moreover, purity of the fractions was also determined with Western blot. The results from the purity determination indicated some contamination in the nuclear fractions, suggesting further optimization of fractionation protocol used. Despite that limitation, the results showed it was possible to use Western blot and the ELISA-based TransAM Nrf2 kit to detect and measure Nrf2 level in different cellular fractions of PBMCs.

Contents

Abbreviations

AMP:	adenosine monophosphate
AOPP:	advanced oxidation protein products
ARE:	antioxidant response element
BSA:	bovine serum albumin
BTB:	broad-complex, tramtrack and bric-à-brac
bZIP:	basic region-leucine zipper
CAT:	catalase
CNC:	cap'n'collar
CPT:	cell preparation tube
CREB:	cyclic AMP responsive element binding protein
CSF:	cerebrospinal fluid
CTR:	C-terminal region
Cul3:	cullin 3
Cy:	cyanine
DGR:	double glycine repeat
DC domain:	domain including DGR and CTR
DTT:	dithiothreitol
ECH:	erythroid cell-derived protein with CNC homology
EDTA:	ethylenediaminetetraacetic acid
ELISA:	enzyme-linked immunosorbent assay
EpRE:	electrophile response element
g:	gravitational force
GAPDH:	glyceraldehyde-3-phosphate dehydrogenase
GC-MS:	gas chromatography-mass spectrometry
GPx:	glutathione peroxidase
GSH:	glutathione
GSR:	glutathione reductase
GSSG:	glutathione disulfide
GST:	glutathione S-transferase
HAT:	histone acetyltransferase
HNE:	4-hydroxnonemal

HO-1:	heme oxygenase-1
HPLC:	high-performance liquid chromatography
HPRT:	hypoxanthine guanine phosphoribosyl transferase
HRP:	horseradish peroxidase
IsoPs:	isoprostanes
IVR:	the intervening region
kDa:	kilodalton
Keap1:	kelch-like ECH-associated protein 1
LDS:	lithium dodecyl sulfate
Maf:	musculo-aponeurotic fibrosarcoma
MDA:	malondialdehyde
MW:	molecular weight
NADPH:	nicotinamide adenine dinucleotide phosphate
NO_2-Tyr:	nitrotyrosine
NP-40:	non-ionic polyoxyethylene
NQO1:	quinone oxidoreductase
Nrf2:	nuclear factor erythroid 2-related factor 2 or nuclear factor (erythroid-derived 2)-like 2
Neh:	Nrf2-ECH homology
NTR:	N-terminal region
OD:	optical density
p300:	transcriptional coactivator with HAT activity
PBMC:	peripheral blood mononuclear cell
PBS:	phosphate-buffered saline
PC:	protein carbonyls
PMNLs:	polymorphonuclear leucocytes
pSS:	Sjögren's syndrome
PVDF:	polyvinylidene difluoride
REAP:	rapid, efficient and practical
RING:	really interesting new gene
RIPA:	radioimmunoprecipitation assay
ROC1:	RING of cullins-1
ROS:	reactive oxygen species
RT:	room temperature

SDS:	sodium dodecyl sulfate
SDS-PAGE:	sodium dodecyl sulfate-polyacrylamide gel electrophoresis
SFN:	sulforaphane
SOD:	superoxide dismutase
tBHQ:	tert-butylhydroquinone
TBS:	tris-buffered saline
TBST:	tris-buffer saline with 0.1% Tween® 20
Ub:	ubiquitin
UV:	ultraviolet
w/v:	weight per volume
WBC:	white blood cell

1. Introduction

Reactive oxygen species (ROS) are continually produced in the body as a result of aerobe metabolism [1]. These molecules are vital for life because they contribute to immune response and are a part of cell signaling pathways [2-4]. In normal cells, ROS level is strictly controlled and balanced by antioxidant defense machinery since a high concentration of ROS is toxic and can potentially damage and modify the cellular components such as lipids, nucleic acid bases, and proteins [5]. However, the balance between the level of ROS and the ability of the body's defense system can be perturbed, which leads to oxidative stress [1, 6]. Oxidative stress is involved in the pathogenesis of many serious diseases [7, 8]. For this reason, the assessment of the oxidative stress level is desired in clinical examination. The most commonly used approaches are measurements of biomarkers, metabolites, and target products of ROS in cerebrospinal fluid (CSF), tissues, blood, and urine. Some biomarkers of oxidative stress are isoprostanes (IsoPs), malondialdehyde (MDA), 4-hydroxnonemal (HNE) from the oxidation of lipids, advanced oxidation protein products (AOPP), nitrotyrosine (NO_2-Tyr), and protein carbonyls (PC) from the protein oxidation [2, 7, 9, 10]. Examples of methods used in detection are high-performance liquid chromatography (HPLC), gas chromatography-mass spectrometry (GC-MS), spectrophotometry, and enzyme-linked immunosorbent assay (ELISA) [7, 10]. Another approach to detect oxidative stress is to measure concentration of the antioxidants glutathione (GSH), catalase (CAT), and superoxide dismutase (SOD). Some efforts to directly detect ROS have also been made using electron spin resonance with spin traps [11]. However, the equipment cost, instability of ROS, lack of specificity and selectivity make the methods less attractive and more challenging in clinical analysis where most test materials are tissues and body fluids [7, 11, 12].

At Stavanger University Hospital, oxidative stress has been studied in some clinical projects. So far, the biomarkers PC, MDA, and AOPP have been used. In one study, both AOPP and MDA concentration increased in patients with IgA nephropathy compared to controls, but their concentrations were also uncovered to be dependent on age and sex [13]. In another study, patients with primary Sjögren's syndrome (pSS) had elevated PC and AOPP level compared to healthy subjects. Nevertheless, no association between the PC or AOPP level and fatigue was found in this study. The outcome was unexpected, as oxidative stress is hypothesized to be a fatigue-induced phenomenon. Fatigue, defined as an overwhelming sense of tiredness, lack of energy, and exhaustion, is a phenomenon often leading to

disablement. Fatigue is also common in patients with chronic inflammatory diseases, and pSS patients were reported to have experienced fatigue [2, 14]. The findings from the studies have raised questions as to whether measurement of PC, MDA, and AOPP alone was sufficient to give a complete picture of oxidative stress status in the body.

In 1994, Moi and colleagues successfully cloned and characterized a gene encoding a protein which was named nuclear factor erythroid 2-related factor 2 (Nrf2) [15]. Nrf2 is today regarded as one of the most important transcription factors in the cellular protection against endogenous and exogenous oxidative stress. Under oxidative stress, activated Nrf2 translocates to the nucleus and heterodimerizes with musculo-aponeurotic fibrosarcoma (Maf). The Nrf2-Maf dimer binds to antioxidant response element (ARE) found in Nrf2 target genes and initiates their expression. The genes expressed encode different enzymes and proteins which protect cells against oxidative damage [16]. Since Nrf2 is ubiquitously expressed in all tissues [17], and there is a clear association between oxidative stress and the increased level of Nrf2 in the nucleus, Nrf2 might be a useful supplementary test which can be used besides PC, MDA, and AOPP. By relatively quantifying cytoplasmic and nuclear levels of Nrf2, the Nrf2-regulated antioxidant defense induced by oxidative stress could be better studied and offer a new approach to assess the oxidative stress status in patients.

The most used method in the investigation of Nrf2 is conventional Western blot. Another used method is ELISA.

The purpose of this project was to compare Western blot and ELISA-based TransAM Nrf2 kit for detection and measurement of Nrf2 levels in PBMCs. Cell cultures have been used in many studies on Nrf2 function, thus *in vivo* studies or studies on cells from individuals are needed. In this study, PBMCs were used as a model system for Nrf2. PBMCs were isolated from blood samples, lysed and subjected to Western blot analysis with three different anti-Nrf2 antibodies. The antibodies detected different epitopes in Nrf2 protein. After the characterization, Western blot was used again to detect Nrf2 in fractions of PBMCs to examine whether it had the same characteristic as in the whole cell lysates. Next, the purity of the cellular fractions was determined, also with Western blot, using antibodies against reference proteins found exclusively in nuclear or cytosolic fractions. Finally, the TransAM kit was used for relative quantifying of Nrf2 level in the cellular fractions (figure 1.1).

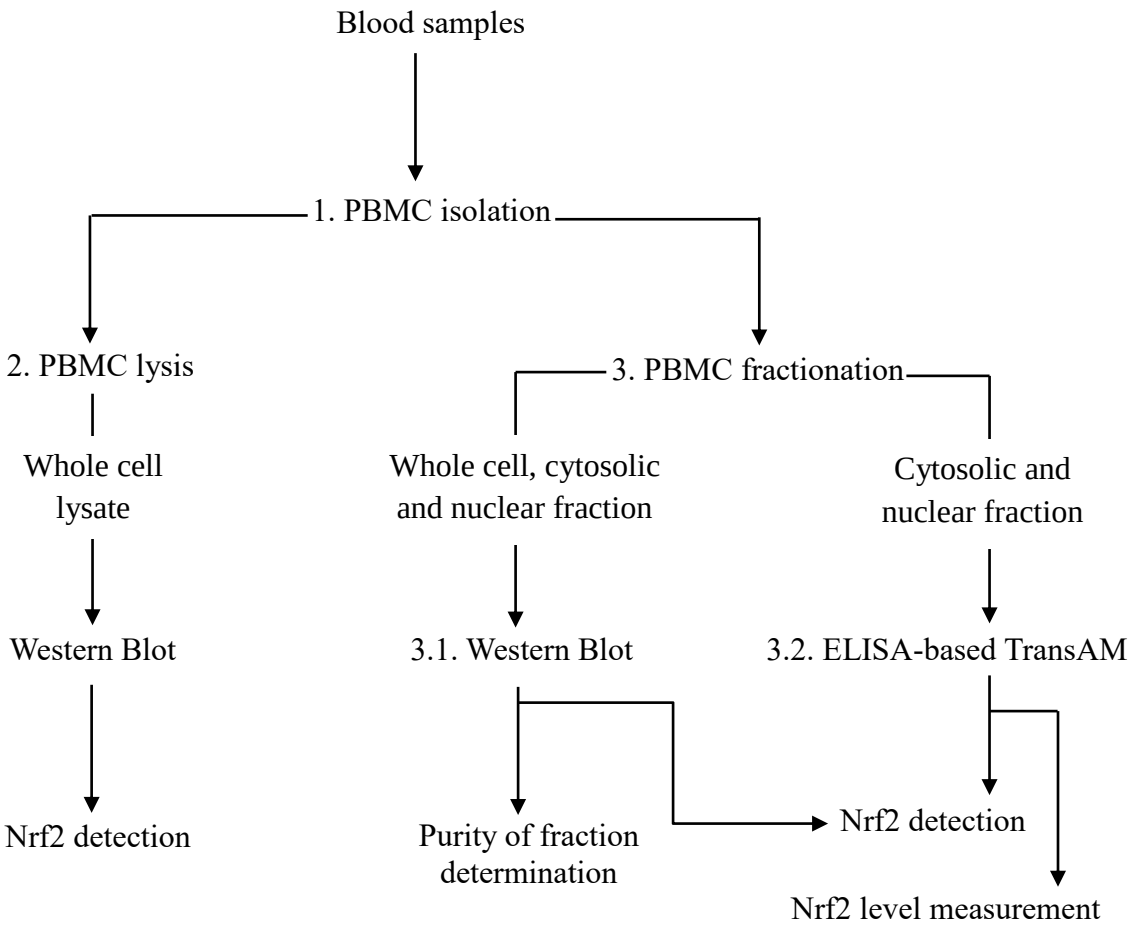

Figure 1.1. Flow chart of the research process in the project. PBMC: Peripheral blood mononuclear cell. Nrf2: Nuclear factor erythroid 2-related factor 2.

2. Theory

2.1 ROS and oxidative stress

Human cells have their own aerobic cellular respiration process in which the inspired oxygen (O_2) is consumed. The physical participation of O_2 takes place in the mitochondrial electron transport chain which has water (H_2O) as one of its final products [18]. However, the O_2 molecules can also be partially reduced instead of completely reduced to H_2O by electrons in the mitochondria. If one single electron is transferred to O_2, superoxide ion ($O_2^{\bullet -}$) is formed. The acquirement of two electrons gives hydrogen peroxide (H_2O_2). Both $O_2^{\bullet -}$ and H_2O_2 are called ROS or oxidants. ROS refer to both free radical and nonradical derivatives of O_2 [1, 19-21] (table 2.1). Free radicals are ROS which contain one or more unpaired electrons [5, 17]. Besides mitochondria, ROS are also produced in microsomes, peroxisomes, and phagocytes [17, 20, 22, 23].

Table 2.1. Some endogenous reactive oxygen species (ROS)

Reactive oxygen species (ROS)	
Free radicals	Nonradicals
Hydroxyl ($^{\bullet}OH$)	Hydrogen peroxide (H_2O_2)
Alkoxyl ($RO^{\bullet}$)	Hypochlorous acid (HOCl)
Peroxyl radicals ($ROO^{\bullet}$)	Peroxynitrite ($ONOO^-$)
Superoxide ion ($O_2^{\bullet -}$)	Organic hydroperoxides (ROOH)

In normal cells ROS are always generated in low and moderate concentrations in a strictly controlled manner as a result of aerobic metabolism [20]. They contribute to many physiological and pathophysiological processes in mammalian cells such as cell growth, cell proliferation, cell survival, defense against infectious agents, and activation of signaling pathways [17, 24-27].

When the concentration of ROS becomes so high that the protective mechanisms inside the body cannot handle, the cells experience a condition called oxidative stress. Since ROS attack lipids, proteins, and DNA in ways that impair and adversely modify cellular

functions [7, 17, 24, 25, 28, 29], oxidative stress is involved in pathogenesis of many conditions and diseases such as ageing, cancer, Alzheimer's disease, Parkinson's disease, Down syndrome, atherosclerosis, diabetes mellitus, ischemia, and rheumatoid arthritis [8, 17, 19, 25].

Oxidative stress can also be caused by xenobiotic factors which are, for example, UV light, cigarette smoking, environmental toxins, medicines, alcohol, and radiation [20, 30, 31].

2.2 Nuclear factor erythroid 2-related factor 2

2.2.1 Machinery for cell protection against oxidative stress

Oxidative stress, whether endogenous or exogenous, is an inevitable challenge for all animal species since aerobic metabolism is entirely dependent on oxygen. Therefore, cells have been equipped with several mechanisms to counteract ROS-induced damages and maintain their redox homeostasis. These mechanisms include the use of antioxidants and antioxidant enzymes, stimulation of endogenous signaling pathways to protect cells from toxic effects of ROS, and reparation of cellular injuries [5, 32].

CAT, SOD, and glutathione peroxidase (GPx) are some representatives of antioxidant enzymes that protect the cells against ROS. Catalase deactivates peroxide, SOD neutralizes $O_2^{\bullet -}$, while GPx catalyzes reactions where peroxides are reduced to alcohols and H_2O by antioxidant GSH [5, 20, 32].

2.2.2 The involvement of Nrf2

Nrf2 regulates the expression of genes coding for antioxidants and antioxidant enzymes in the machinery against oxidative stress [33]. Nrf2 is a member of the cap'n'collar (CNC) subfamily of the basic region-leucine zipper (bZIP) transcription factor protein family [15, 34-36]. The protein is characterized by typical bZIP motif and a CNC domain. It is present not only in vertebrates but also in invertebrates and can be found ubiquitously in all tissues with different levels of expression. The gastrointestinal tract, liver, kidney, and lungs have a relatively high expression level of Nrf2 [17, 34, 37]. Nrf2 consists of six domains

Nrf2-ECH (erythroid cell-derived protein with CNC homology) homology (Neh1-Neh6) that are well conserved and have different functionalities [38-40] (figure 2.1A).

Under normal and unstressed conditions, Nrf2 is sequestered and degraded by proteasome in the cytoplasm by ubiquitination, which is mediated by kelch-like ECH-associated protein 1 (Keap1) [39, 41-46] and cullin 3 [47-50].

Keap1 was first described by Itoh, Wakabayashi et al. (1999) as a Nrf2 negative regulator in the cytoplasm [39]. Keap1 is a zinc finger protein [38] belonging to the broad-complex, tramtrack, and bric-à-brac (BTB)-Kelch protein family [51]. Keap1 comprises the N-terminal region (NTR), BTB domain, the intervening region (IVR), the double glycine repeat (DGR) or Kelch repeat, and the C-terminal region (CTR) [52-54]. DGR and CTR constitute the DC domain in Keap1 [17, 53, 55] (figure 2.1B). The protein resides mainly in the cytoplasm as homodimer dimerized through its BTB domain, but a small amount of Keap1 is also localized in the nucleus and the endoplasmic reticulum (ER) [55, 56].

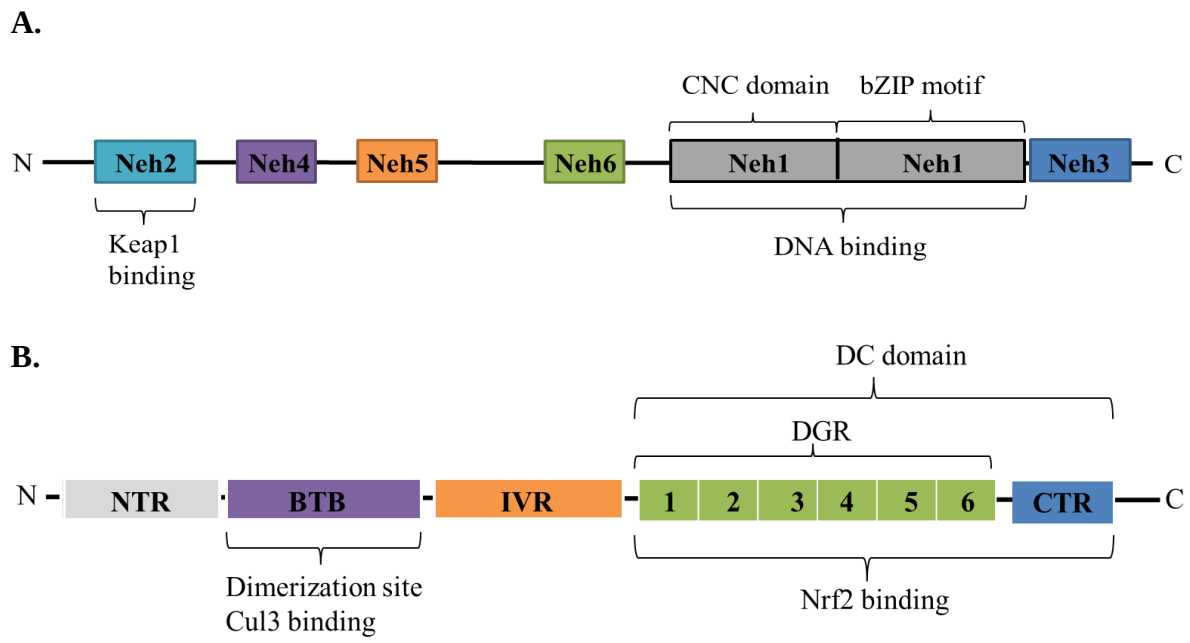

Figure 2.1. The domain structures of Nrf2 (A) and Keap1 (B).

Interaction between Nrf2 and functional Keap1 homodimer [57] takes place at the N-terminal Neh2 domain and the DC domain in the Nrf2 protein and the Keap1 protein respectively [39, 55]. The DC domain binds to the Neh2 domain via either DLG or ETGE, two different motifs found within the Neh2 domain of Nrf2 (figure 2.2).

Cullin 3 (Cul3) associates with the BTB and IVR region in the Keap1 at the N-terminal domain [47, 48, 50, 58]. Cul3 binds to the ROC1 (really interesting new gene (RING) of Cullin) protein at C-terminal domain [47], resulting in a protein complex called ubiquitin ligase. Ubiquitin ligase facilitates the transfer of ubiquitin (Ub) from ubiquitin-conjugating enzyme to substrate protein [59] (figure 2.2).

Since Keap1, and not Cul3, binds directly to Nrf2, Keap1 functions as an adaptor molecule of the Cul3-RING ligase [48-50] (figure 2.2).

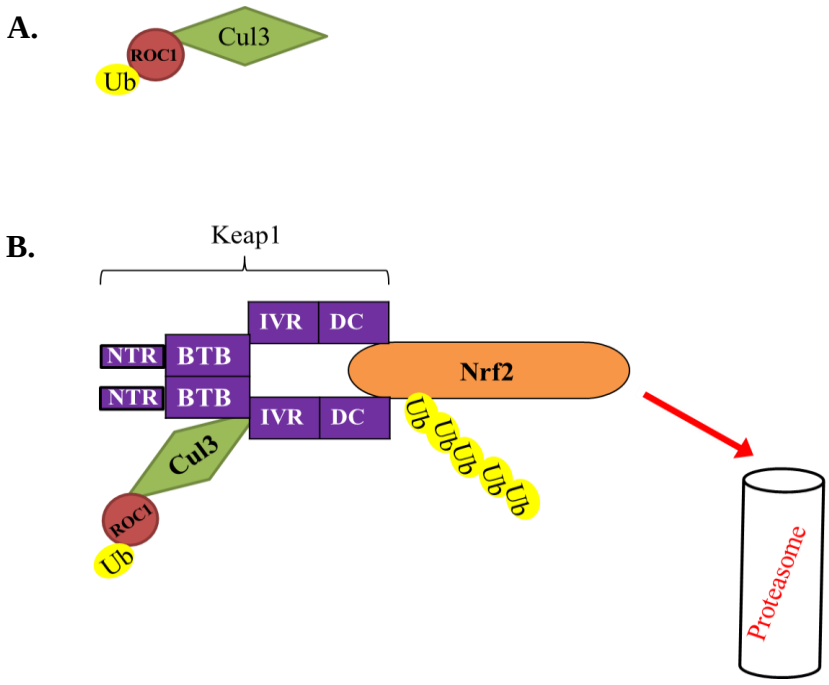

Figure 2.2. Models depicting structure of ubiquitin ligase (A) and Nrf2 regulation by Keap1 and Cul3 (B). Keap1 homodimerizes via its BTB domains. The two DC domains in the Keap1 homodimer bind to one Nrf2 molecule. BTB and IVR region in the Keap1 associate with the Cul3 in the ubiquitin ligase.

Upon exposure to oxidative stress, Keap1 residues sense the abnormal changes and undergo diverse modifications [38, 43, 60]. These modifications result in disruption of the Keap1-Nrf2 association, thus preventing Nrf2 ubiquitination and degradation, which liberates Nrf2 and allows it to translocate into the nucleus [39, 56, 60].

In the nucleus, Nrf2 forms a heterodimer with small protein Maf [61]. The Nrf2-Maf dimer binds to ARE [62], also referred to as electrophile response element (EpRE) [63] in the promoter regions of target cytoprotective genes [64]. In addition, the Nrf2-Maf dimer recruits other transcription coactivators such as CREB (cyclic AMP responsive element binding protein) binding protein (CBP) and p300 [65-67], resulting in a broader transcriptional response [68, 69] (figure 2.3).

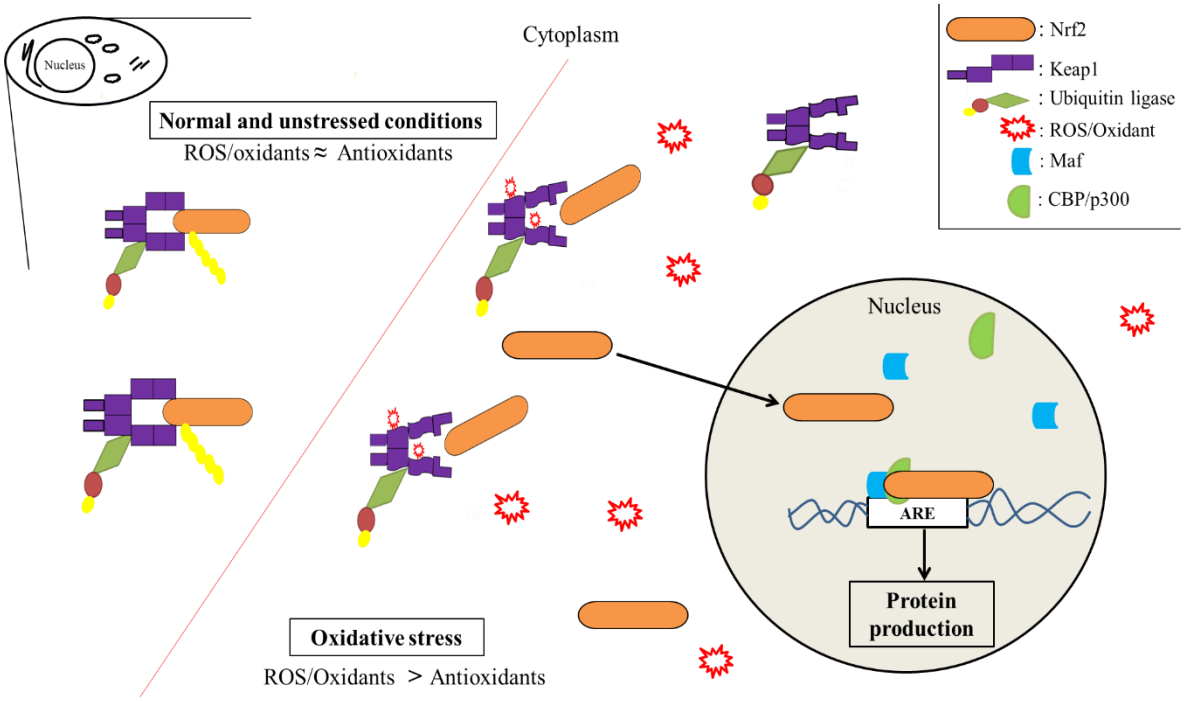

Figure 2.3. Under normal and unstressed conditions, Nrf2 is repressed by Keap1 and subsequently degraded. If Keap1 senses oxidative stress, Nrf2 is liberated and activated. Then, Nrf2 translocates to the nucleus and binds to Maf, CBP, and p300. The complex binds to ARE found in Nrf2 target genes and initiates the expression of those genes.

In studies utilizing homozygous Nrf2-deficient mouse model ($Nrf2^{-/-}$), researchers have found that the induction of CAT [70], SOD [70], GSR [71] and GPx [72] are mediated by Nrf2 through the Nrf2-ARE pathway, yet are dependent on cells and organs used as material. Akino et al. (2018) in their research with human luteinized granulose cells from ovarian follicles have additionally demonstrated that depletion of endogenous Nrf2 resulted in a significant decrease in protein expression of CAT and SOD [73].

Additionally, Nrf2 also plays a key role in regulation of phase II detoxifying enzymes through ARE [74, 75]. Such phase II detoxifying enzymes are glutathione S-transferase

(GST), NAD(P)H: quinone oxidoreductase (NQO1), and heme oxygenase (HO-1) [36, 69, 76]. Lee et al. (2003) have also identified many of Nrf2-dependent genes in their research with mouse primary astrocytes using oligonucleotide microarray analysis. These genes enconde, among other things, growth factors, signaling proteins, and metabolic enzymes [77].

Relation between ROS, oxidative stress, antioxidants and Nrf2 is summarized in figure 2.4.

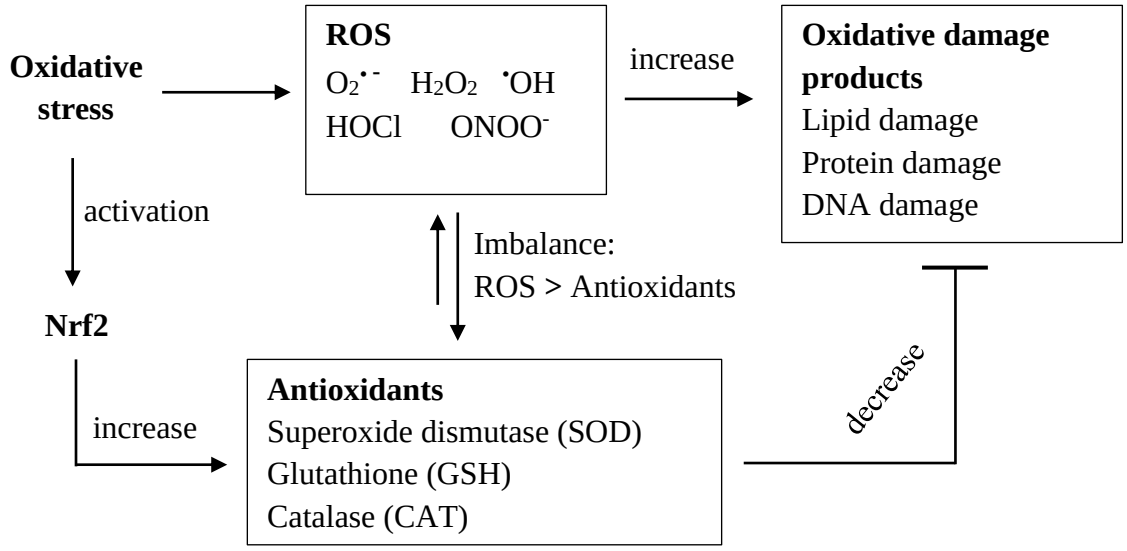

Figure 2.4. Relation between ROS, oxidative stress, antioxidants and Nrf2 in stressed cells.

2.3 White blood cells and PBMCs

The white blood cells (WBCs), also called leucocytes, are one of three main components of the blood system besides red blood cells (RBCs)/erythrocytes and thrombocytes/platelets.

The WBCs are divided into three different types: granulocytes, monocytes, and lymphocytes. Granulocytes comprise neutrophils, eosinophils, and basophils. They have, in addition to granular cytoplasm, segmented nuclei with varying shapes. Therefore, they are often referred to as polymorphonuclear leucocytes (PMNLs) [78-81]. Monocytes and lymphocytes, on the contrary, have neither cytoplasmic granules nor multi-lobed nuclei and thus are called peripheral blood mononuclear cells (PBMCs) [81-83]. The WBCs do not have hemoglobin, but they contain the same organelles, such as mitochondria, Golgi apparatus, nucleus, ER, and ribosomes as other eukaryote cells [79, 81]. Monocytes are the largest

peripheral blood cells whose diameter is 10-18 µm, while lymphocytes are the smallest ones measuring 10-14 µm in diameter [84].

White blood cells are inflammatory cells [85] which defend the body against harmful, non-self or foreign agents and eliminate degraded components of self [80, 83]. These functions have been shown to be associated with the Keap1-Nrf2 pathway. Nrf2 in WBCs are activated by inflammatory related molecules such as prostaglandins and nitric oxide (NO). Since Nrf2 suppress accumulation of ROS generated by the NADPH oxidase complex in macrophages and neutrophils, their expression exerts anti-inflammatory effects, inhibits tumor metastasis and attenuates protection of tumor cells. Research on Nrf2-deficient mice also indicated that Nrf2 regulates phagocytosis [86].

2.4 Principle of Western blot

Western blot (WB) is a technique used to detect and identify specific proteins in a protein mixture [87]. The proteins are separated by gel electrophoresis and subsequently transferred from the gel to a membrane for detection using specific polyclonal or monoclonal antibodies. The specificity of the antibody-antigen (proteins, or part of them) interaction is therefore important.

2.4.1 Protein separation by gel electrophoresis

Gel electrophoresis is a method used for analytical separation of proteins in a mixture. The size of molecules of current interest determines the concentration of gel material and the size of pores in the gel [19, 88]. In this project, sodium dodecyl sulphate-polyacrylamide gel electrophoresis (SDS-PAGE), a variant of gel electrophoresis, was utilized. In SDS-PAGE, the loading buffer contains anionic detergent such as SDS (CH_3-$(CH_2)_{10}$-$CH_2OSO_3^-Na^+$) or LDS (CH_3-$(CH_2)_{10}$-$CH_2OSO_3^-Li^+$) and reducing agent; either dithiothreitol (DTT) or β-mercaptoethanol (2-thioethanol). LDS has a better solubility than SDS at low pH and temperature [89]. The detergent denatures native proteins by disrupting nearly all noncovalent interactions found in them, while the reducing agent is added to reduce disulfide bridges that participate in proteins' tertiary structure [19, 20, 88]. Since the LDS-denatured protein complexes have a strong negative charge which is proportional to the mass of the protein, they will move towards the anode down to the bottom of the gel when an electrical

current is applied. The velocity of migration depends on size or mass of the proteins, electrical field strength, and concentration of gel material. If the last two factors are constant, the separation of the molecules is be related solely to their size. The smallest molecules will move faster due to molecular sieving effect in the gel [19, 88]. The polyacrylamide gel used in SDS-PAGE consists of two types of gel: a stacking gel that has high porosity to concentrate the proteins, resulting in sharp bands and a separating gel with a higher concentration of polyacrylamide, meaning lower porosity, thus separating the proteins based on their sizes [88].

2.4.2 Protein detection

Prior to protein detection in Western blot by chemiluminescence or fluorescence the following three steps are performed [19, 87, 88, 90, 91]:

1) Blotting: The separated proteins migrate out of the gel onto a membrane when an electric current is applied at a 90 degrees angle to the gel.

2) Blocking: The membrane is blocked to prevent non-specific binding between the detection antibody and the remaining protein binding sites of the membrane because the antibody, in essence, is also protein. There are many blocking agents that can be employed; for example, bovine serum albumin (BSA), skim milk powder, fetal calf serum, Tween 20, or gelatin.

3) Antibody incubation: The membrane is incubated first in a primary antibody and then in a secondary antibody. The primary antibody has the function of detecting the protein of interest because of its specificity for the target protein or part of target protein. The secondary antibody, on the other hand, is specific to the first antibody and therefore binds directly to it. When this has happened, a sandwich structure is formed. The secondary antibody is conjugated with either an enzyme or a fluorophore, allowing subsequent detection in an imaging system.

Chemiluminescence

The secondary antibody is conjugated with enzyme horseradish peroxidase (HRP). The membrane is incubated in substrate for HRP. The reaction between the substrate and HRP produces chemiluminescence which is detected by camera in an imaging system (figure 2.5A). The luminescence signal is proportional to the amount of the target protein.

Fluorescence

The secondary antibodies used are conjugated to fluorophores or fluorescent dyes such as cyanines (Cy2, Cy3 and Cy5) (figure 2.5B). A fluorophore is excited when it absorbs light from the light source at a specific excitation wavelength. The excitation leads to the subsequent emission of radiation or fluorescence in form of visible light at its specific emission wavelength when the fluorophore returns to the ground state. The fluorescent signal which visualizes the proteins of interest is then detected by a sensitive digital camera in the imager [88, 92]. The signal is proportional to the amount of the target protein. A benefit of fluorescent Western blot is the ability to examine multiple proteins simultaneously on a membrane, called multiplex detection, by utilizing primary antibodies from different host species (rabbit, mouse or rat) and secondary antibodies conjugated to fluorophores with different wavelengths for each of the primary antibodies [90].

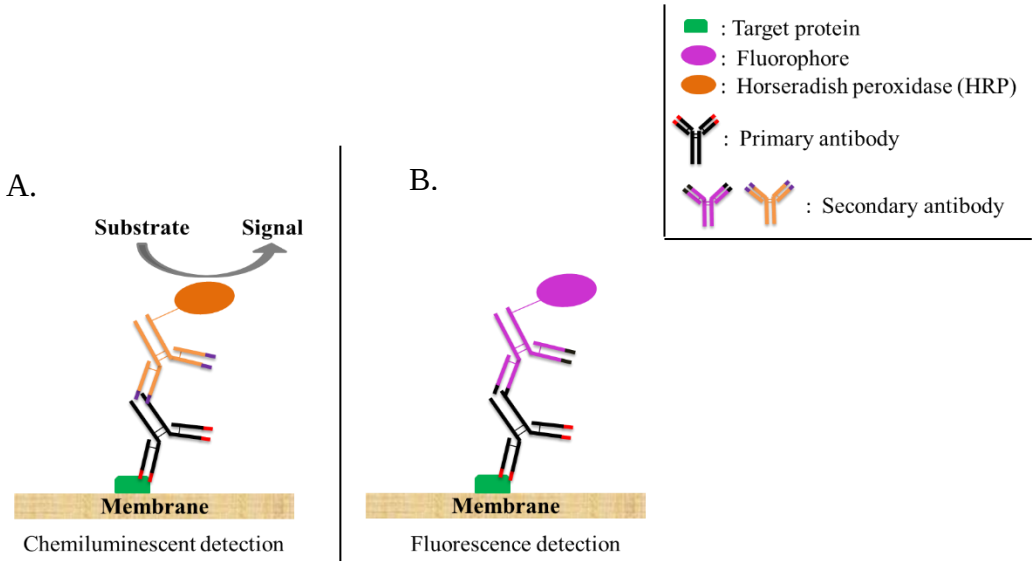

Figure 2.5. Principle of chemiluminescent (A) and fluorescent detection (B) in Western blot.

2.5 Principle of ELISA and ELISA-based TransAM Nrf2 kit

ELISA is technique used to detect and quantify a protein colorimetrically. The technique relies on the formation of antigen-antibody complex followed by detection of its presence by addition of substrate of report enzyme [19, 20, 88].

The ELISA-based TransAM Nrf2 kit (Active Motif, Carlsbad, CA) used in this project employs this principle to detect Nrf2.

The wells are precoated with immobilized oligonucleotide containing the ARE consensus binding site (5'-GTCACAGTGACTCAGCAGAATCTG-3') which functions as capturer for Nrf2. Nrf2 in samples will bind to the capturer and become trapped. Nrf2 operates henceforth as an antigen for a primary antibody added in the next step. Subsequently, an anti-species antibody, called secondary antibody, which is specifically against the primary antibody is used. The secondary antibody is already conjugated with the enzyme HRP. Thus, when an enzyme substrate is added in the final step, the ARE-bound Nrf2/primary antibody/secondary antibody complex produces color whose absorbance at a particular wavelength is measured in a spectrophotometer (figure 2.6). The intensity of the color product is used to assess the abundance of Nrf2 detected [19, 20, 88, 93].

For analysis of positive control in the kit, competitive ELISA is employed. The coated capturer in the wells competes with either wild-type or mutated consensus oligonucleotide, for binding to Nrf2 in test samples. Since the competitive capturers are mobilized, the complex formed between it and Nrf2 is easily removed in washing steps. As a result, the signal from the target Nrf2 is decreased in detection, which indicates that a prevention of Nrf2 binding to the precoated antibody in the plate has occurred.

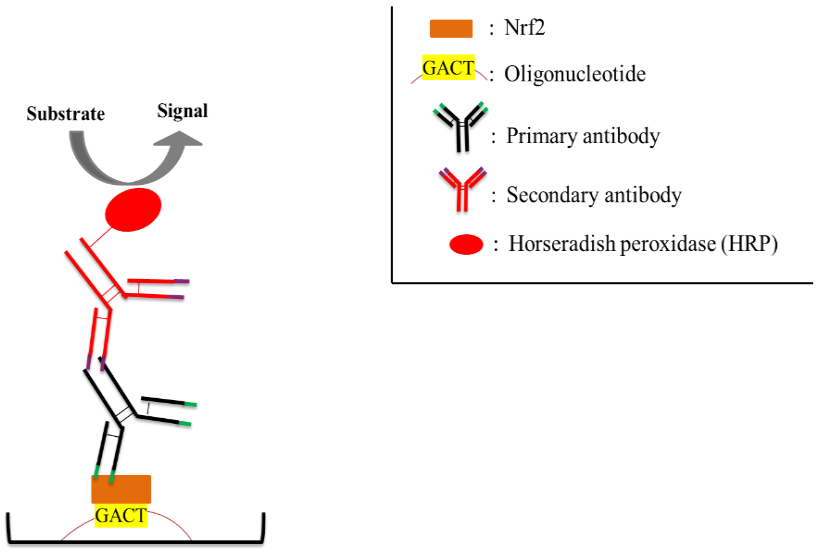

Figure 2.6. Principle of ELISA-based TransAM Nrf2 kit

3. Materials and methods

3.1 Materials

3.1.1 Chemicals

Sample preparation

Cell preparation tube (CPT) with sodium citrate, 8mL from BD Biosciences, New Jersey, USA.

Microtainer® tube with no additive (red) from BD, New Jersey, USA.

NP-40 (nonidet-P40, aqueous detergent solution 10% (w/v), catalog number: 28324, lot number: OD183328) from Thermo Fisher Scientific, Rockford, Illinois, USA.

Phosphate-buffered saline (PBS) packs (0.1 M sodium phosphate, 0.15 M sodium chloride, pH 7.2 dissolved in a final volume of 500mL deionized water) from Thermo Fisher Scientific, Rockford, Illinois, USA.

Trizma® base (hereafter referred to as Tris base) from Sigma-Aldrich, Steinheim, Germany

Sodium chloride (NaCl) from VWR International AS, Leuven, Belgium

Sodium deoxycholate from Sigma-Aldrich, Steinheim, Germany

Sodium dodecyl sulfate (SDS), for molecular biology, approx. 99% from Sigma-Aldrich, Steinheim, Germany.

Bradford Assay

Bradford reagent (for detection of the total protein concentration with the range of 0.1-1.4 mg/mL) from Sigma-Aldrich, Steinheim, Germany.

Bovine serum albumin (BSA, heat shock fraction, protease free, fatty acid free, essentially globulin free, pH 7, ≥ 98%) from Sigma-Aldrich, Steinheim, Germany.

Polystyrene microplate, clear, flat bottom (catalog number: 655101, lot number: E140716F and E100301J) from Greiner Bio-One, Frickenhausen, Germany.

Western Blot

SDS-PAGE/Gel electrophoresis

Bolt™ 10% bis-tris plus gels (1.0 mm x 12 wells) (hereafter referred to as bolt gel) from Life Technologies, Invitrogen by Thermo Fisher Scientific, Carlsbad, California, USA.

Bolt™ sample reducing agent (10 x) from Life Technologies, Invitrogen by Thermo Fisher Scientific, Carlsbad, California, USA.

Bolt™ MOPS SDS running buffer (20x) from Life Technologies, Invitrogen by Thermo Fisher Scientific, Carlsbad, California, USA.

Pageruler™ plus prestained protein ladder from Thermo Fisher Scientific, Rockford, Illinois, USA.

Supersignal™ molecular weight protein ladder from Thermo Fisher Scientific, Rockford, Illinois, USA.

Pierce™ lithium dodecyl sulfate (LDS) sample buffer non-reducing (4 x) from Thermo Fisher Scientific, Rockford, Illinois, USA.

Dithiothreitol (DTT, BioUltra, for molecular biology, ≥99.5% (RT)) from Sigma-Aldrich, Steinheim, Germany.

Protein detection

1-step™ transfer buffer, Western blotting filter paper (7cm x 8.4cm, thickness: 0.83mm) from Thermo Fisher Scientific, Rockford, Illinois, USA.

Polyvinylidene difluoride (PVDF) transfer membrane (0.45 µm, 26.5 cm x 3.75 m roll for western blotting applications) from Thermo Fisher Scientific, Rockford, Illinois, USA.

Rabbit anti-HPRT monoclonal primary antibody (catalog number: ab133242, lot number: GR97370-7) from Abcam, Cambridge, UK.

Mouse anti-GAPDH monoclonal primary antibody (catalog number: ab9484, lot number: GR174666-7) from Abcam, Cambridge, UK.

Rabbit anti-Nrf2 (C-term) polyclonal primary antibody (catalog number: 10214) from Cayman Chemical, Michigan, USA.

Rabbit anti-Nrf2 (N-term) polyclonal primary antibody (catalog number: 14114, batch: 0480703-1) from Cayman Chemical, Michigan, USA.

Mouse anti-Lamin B1 (L-5) monoclonal primary antibody (catalog number: 33-2000, lot number: QG215256) from Thermo Fisher Scientific, Rockford, Illinois, USA.

Supersignal™ west femto maximum sensitivity substrate from Thermo Fisher Scientific, Rockford, Illinois, USA.

Rabbit anti-Nrf2 polyclonal primary antibody (catalog number: 61599, lot number: 25414001) from Active Motif, La Hulpe, Belgium.

Goat anti-rabbit IgG conjugated to HRP polyclonal secondary antibody (catalog number: 15015, lot number: 27117008) from Active Motif, La Hulpe, Belgium.

Goat anti-mouse IgG, peroxidase conjugated, H+L polyclonal secondary antibody (catalog number: AP124P, lot number: 2966512) from Merck Millipore, Massachusetts, USA.

Tween® 20 (Polysorbate), technical from VWR, Fontenay-sous-Bois, France.

Ponceau S solution (BioReagent, suitable for electrophoresis, 0.1 % (w/v) in 5% acetic acid) from Sigma-Aldrich, Steinheim, Germany.

Benzonase® nuclease (≥ 250 unites/µL, ≥ 90% (SDS-PAGE), recombinant, expressed in E.coli, buffered aqueous glycerol solution) from Sigma-Aldrich, Steinheim, Germany.

Glycine (for electrophoresis, ≥ 99%) from Sigma-Aldrich, Steinheim, Germany.

BSA (heat shock fraction, protease free, fatty acid free, essentially globulin free, pH 7, ≥ 98%) from Sigma-Aldrich, Steinheim, Germany.

Methanol, for analysis from Merck, Darmstadt, Germany

Skim milk powder, for microbiology from Merck, Darmstadt, Germany

Hydrochloric acid (HCl) fuming 37%, for analysis from Merck, Darmstadt, Germany

AzureSpectra rb650/ms550 western kit, with fluorescent block from Azure Biosystems, Dublin, California, USA

TransAM Nrf2 kit (hereafter referred to as TransAM) from Active Motif, La Hulpe, Belgium.

3.1.2 Equipment

Bradford assay and ELISA

Synergy H1 microplate reader for measurement of absorbance of proteins from BioTek, Vermont, USA.

Western blot

XCell surelock™ mini-cell electrophoresis system for gel electrophoresis from Life Technologies, Invitrogen by Thermo Fisher Scientific, Carlsbad, California, USA.

Pierce power blotter system and Pierce power blot cassette for electrotransfer of separated proteins from gel onto activated PVDF membrane from Thermo Fisher Scientific, Rockford, Illinois, USA.

Azure c400 imaging system for blot image acquisition from Azure Biosystems.

3.2 Methods

PBMCs from blood samples were isolated using two different methods, one provided by the manufacturer of CPTs (method 1) and one developed at the laboratory of Stavanger University Hospital (method 2). The yield of isolated PBMCs of the two methods were compared to find out the method with highest yield. For the comparison, two parameters used were: 1) total number of isolated PBMCs and 2) total protein concentration in isolated PBMCs.

Initially, Nrf2 was characterized in cell lysates of isolated PBMCs in Western blot using three different anti-Nrf2 antibodies. After the characterization, PBMCs were fractionated to obtain whole cell, cytosolic, and nuclear fractions. Western blot was used again to detect Nrf2 in the fractions and to determine their purity. The purity determination and Nrf2 detection were performed simultaneously. For the purity determination, antibodies against Lamin B1, which is the nuclear reference protein, HPRT and GAPDH, which are the cytosolic reference proteins, were employed. In addition to Western blot, the ELISA-based TransAM was used to detect and measure Nrf2 level in cytosolic and nuclear fraction (figure 1.1, page 8).

3.2.1 Sample preparation

3.2.1.1 Isolation of PBMCs

Blood from volunteers was collected in CPTs and subsequently centrifuged at 1,600 x *g* for 30 minutes at room temperature (RT) (figure 3.1) in a swing-out bucket rotor.

Method 1

The method followed the protocol provided by BD Biosciences in product insert for CPT with sodium citrate.

Immediately after centrifugation, the upper half of the plasma was discarded. The residual, including an undisturbed cell layer, was transferred to a new 15 mL conical centrifuge tube with cap. The final volume in the tube was brought up to 15 mL by adding ice-cold PBS. The tube was inverted 5 times and subsequently centrifuged for 15 minutes at 300 x *g* at RT for washing. After the centrifugation, supernatant was discarded, and cell pellet

was resuspended in the remaining PBS. The cell pellet was mixed with 10 mL ice-cold PBS followed by a centrifugation at 300 x *g* for 10 minutes at RT. After centrifugation, as much supernatant as possible was removed without disturbing the cell pellet, and the cell pellet was resuspended in the remainder of PBS for further procedure.

Method 2

Immediately after centrifugation, the entire content of the tube above the gel was poured into a new 15 mL conical centrifuge tube with cap in order to homogenize mononuclear cells and plasma. The tube was subsequently centrifuged for 10 minutes at 4 °C at 200 x *g* (program 1). After centrifugation, as much supernatant as possible was discarded without disturbing the cell pellet. The cell pellet was then washed 2 times, each in 10 mL ice-cold PBS followed by centrifugation using program 1 and the removal of supernatant. Thereafter, the cells were dissolved in the remaining PBS. They were then transferred into a new Eppendorf tube and placed on ice. Cells which were not used on the same day were stored at -80 °C.

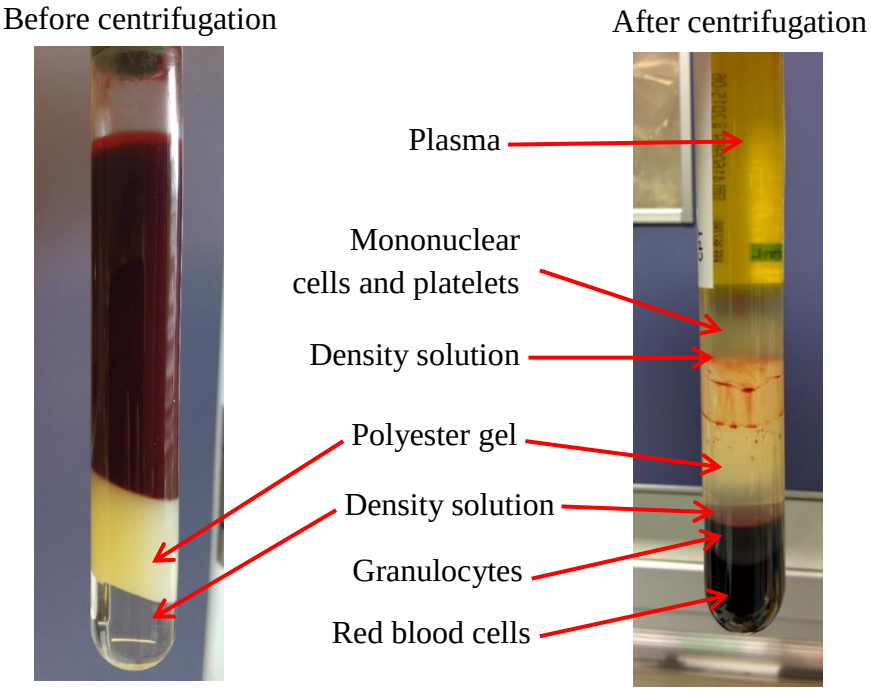

Figure 3.1. Layer of elements formed in CPTs before and after centrifugation.

3.2.1.2 Cell lysis

Prior to the preparation of the cell lysate, the volume of isolated cells was determined. The isolated cells were then dissolved completely in RIPA buffer in a ratio of 1:1 (See Appendix 2: Solutions for detailed recipe). The cells-RIPA mixture was incubated on ice for 40 minutes followed by centrifugation at 13,000 x *g* for 15 minutes at 4 °C. The supernatant was transferred into a new tube for further analysis. The cell pellet was discarded.

3.2.1.3 Cell fractionation

The procedure was adopted from the protocol "Rapid isolation of nuclei from cells in vitro" where a rapid, efficient and practical (REAP) method was described by Nabbi and coworkers (2015) [94]. Some modifications have, however, been made to adapt fractionation for PBMCs.

The cell pellets obtained after isolation were resuspended in 300 µL ice-cold PBS for washing. The mixture was centrifuged at 9,391 x *g* for 13 seconds at RT. After centrifugation, the supernatant was removed, and the cell pellet was resuspended in 300 µL ice-cold 0.1% NP-40 in PBS (See Appendix 2: Solutions for detailed recipe) and triturated several times using a p1000 micropipette. 100 µL of the cell suspension was transferred into a new Eppendorf tube and designated as "whole cell" fraction. The residual cell suspension was centrifuged at 9,391 x *g* for 13 seconds at RT. The obtained supernatant was thereafter transferred into a new Eppendorf tube and named as "cytosolic" fraction. The remaining pellet was resuspended for the second time in 300 µL ice-cold 0.1% NP-40 in PBS. After being centrifuged as mentioned above, the supernatant was discarded, and the pellet was labelled as "nuclear" fraction (figure 3.2) [94].

1. Cell washing

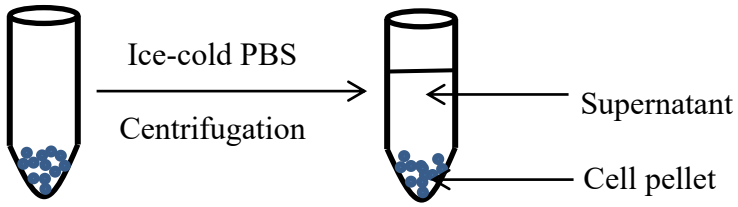

1. Whole cell fraction collection

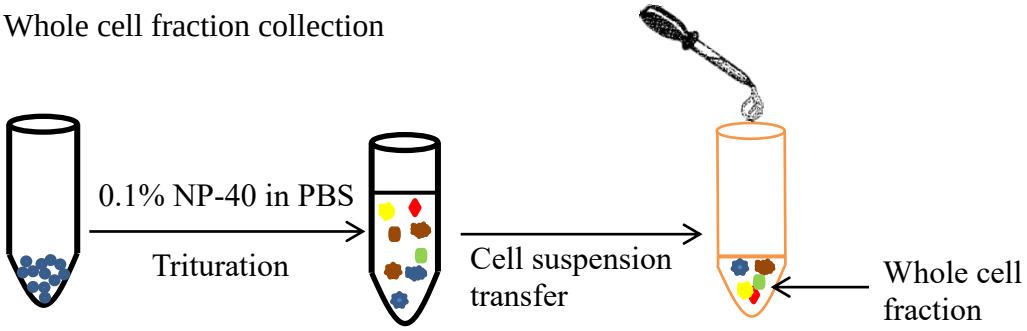

2. Cytosolic fraction collection

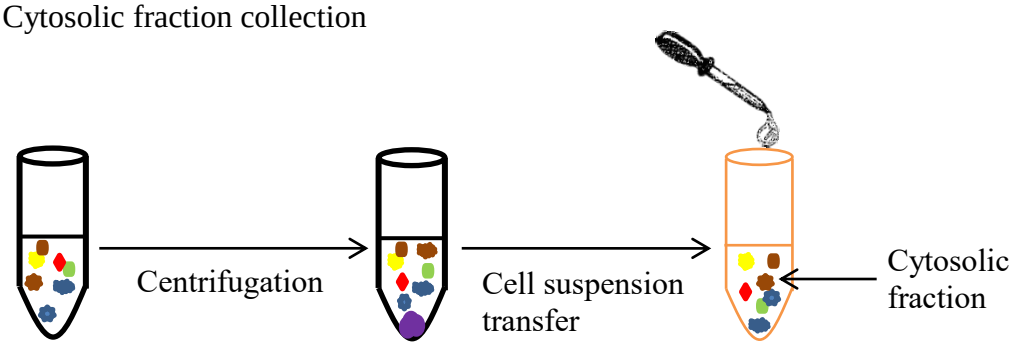

3. Nuclear fraction collection

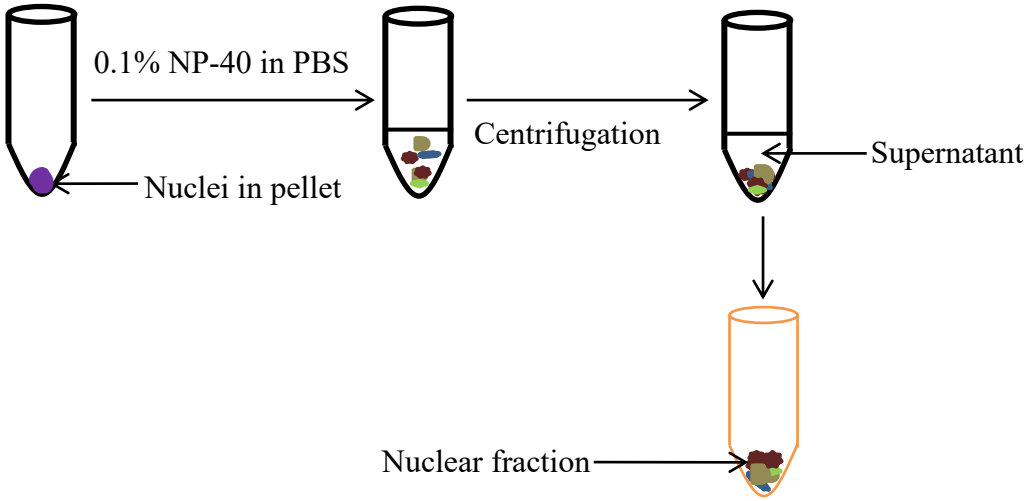

Figure 3.2. Four steps in the protocol for REAP cell fractionation, which gives three final products: whole cell, cytosolic, and nuclear fraction.

3.2.2 Evaluation of isolation of PBMCs

PBMCs were isolated from six vials from one person, three by method 1, and three by method 2. One portion of each isolated cell sample was used in the counting of the total number of isolated PBMCs, and the rest was used in protein concentration determination.

For cell counting, the isolated cell sample was diluted at 1:100 in PBS in microtainer tube with no additive. Flow cytometry was employed. The method measured intensity of fluorescence and scattered light of each component in the sample when it passed through a laser beam [83, 88].

For protein concentration determination, PBMCs were first lysed in RIPA buffer, then the protein concentration was measured with a Bradford assay.

Bradford assay for protein quantitation

Establishment of calibration standard curve

One gram dry BSA was dissolved in 10 mL ultrapure water to make a stock solution of 100 g/L BSA. From the 100 g/L (= 100 mg/mL) BSA solution, a concentration series from 0.15 mg/mL to 1.3 mg/mL was prepared (table 3.3).

Table 3.3: BSA dilution series for Bradford calibration standard curve

Standard	BSA concentration (mg/mL)	BSA stock solution (µL)	PBS (µL)
1 (Blank)	0	0	5000
2	0.15	7.5	4992.5
3	0.3	15	4985
4	0.6	30	4970
5	0,9	45	4955
6	1.3	65	4935

96 well plate assay

The Bradford reagent was gently mixed and equilibrated to RT before use. The protein concentration was measured according to the manufacturer's protocol. Samples were diluted in PBS prior to the measurement. In different wells, 5 µL of blank, 5 µL of each standard, and 5 µL of each diluted sample were added in triplicates. 250 µL of the Bradford

reagent was added into each well. After 25 minutes mixing on a microplate shaker at RT, absorbance at 595 nm was measured in Synergy H1 microplate reader.

3.2.3 Western blot

3.2.3.1 Characterization of Nrf2 in lysed PBMCs

Sample preparation

Ten µg of total protein was loaded per well in SDS-PAGE. The volume of each lysate used was determined according to formula 1:

$$Volume\ (\mu L) = \frac{10\ \mu g}{Protein\ concentration\ (\mu g/\mu L)} \qquad \text{(Formula 1)}$$

The loading buffer containing LDS (4x) and DTT (10x) were added to each loading lysate. The sample was then heated for 10 minutes at 70 °C and subsequently spun down briefly for 2-3 seconds before loading on a bolt gel.

SDS-PAGE

500mL of Bolt™ MOPS SDS running buffer (20x) was prepared by adding 25 mL of the running buffer in 475 mL ultrapure water. The bolt gel was run for 55 minutes at 160 V and 1 hour at 150 V.

Blotting

PVDF membrane was activated in methanol for about 1 minute and washed with ultrapure water 3 times, each time for 15 seconds. Afterwards, the membrane and four sheets of filter paper were equilibrated in transfer buffer for 10 minutes with gentle agitation. Instructions from Thermo Fisher Scientific for gel-to-protein transfer of proteins in the Pierce power blotter system was followed. The transfer of proteins to the membrane was then verified using Ponceau S staining [95].

Blocking

Before blocking, the membrane was washed thoroughly in 1 x tris-buffered saline (TBS) several times to get rid of the color from Ponceau S staining. The membrane was blocked with 15 mL blocking buffer for 1 hour at RT with gentle agitation. After blocking,

the membrane was washed 3 times for 5 minutes per wash with 1x tris-buffer saline with 0.1% Tween® 20 (TBST). Preparation of the blocking buffer, TBS and TBST are described in detail in Appendix 2: Solutions.

Antibody incubation

After blocking and washing, the membrane was incubated in anti-Nrf2 primary antibody, diluted at 1:1,000 in milk (3% weight per volume (w/v)) solution, for 2 hours at RT with gentle agitation (recipe for milk (3% (w/v)) solution is provided in Appendix 2: Solutions). The membrane was washed 3 times for 5 minutes per wash with 1x TBST and subsequently incubated in anti-rabbit IgG HRP-conjugated secondary antibody diluted at 1:30,000 in milk (3% (w/v)) solution for 1 hour at RT with gentle shaking. After incubation, the membrane was washed 3 x 5 minutes per wash with 1x TBST before protein detection.

Chemiluminescent protein detection

Following the washes in TBST, the membrane was incubated for 5 minutes in detection solution which was the substrate for the enzyme HRP according to the manufacturer's instructions. Excess substrate was drained off after the incubation. The membrane was then covered by two transparent and clean plastic sheets. Any trapped air bubbles were removed. The membrane was exposed in the Azure c400 imaging system.

Secondary antibody control

To determine non-specific signals derived from secondary antibody, a lysate was subjected to Western blot where it was incubated with only anti-rabbit IgG HRP-conjugated secondary antibody. The incubation with primary antibody was omitted.

3.2.3.2 Nrf2 detection in cellular fractions and purity determination

Chemiluminescent detection

All obtained nuclear fraction was used. Amount of whole cell and cytosolic fraction used was 65 µL. To reduce viscosity in the nuclear fraction caused by release of chromosomal DNA, 1 µL benzonase nuclease was added, followed by an incubation at 37 °C for 30 minutes for nucleic acid digestion.

The Western blot protocol employed was described above. Loading buffer was added to each loading fraction. The bolt gel was run for 63 minutes at 140 V.

To control the purity of fractions, HPRT, GAPDH and Lamin B1 were detected in addition to Nrf2. Since anti-Nrf2 antibody and anti-HPRT antibody were produced in rabbits, while anti-Lamin B1 antibody and anti-GAPDH antibody were produced in mice, each membrane was cut horizontally into two parts prior to the detection to prevent cross-reactivity. Antibody dilutions are presented in table 3.4.

GAPDH and Lamin B1 in the same fractions were detected after the previously used primary and secondary antibodies were removed from the current membrane by stripping. The membrane was incubated twice in glycine-HCl stripping solution at RT for 10 minutes, followed by washing with PBS (2 x 10 minutes) and with TBST (2 x 5 minutes) with gentle shaking. After the removal av TBST, the membrane was re-blocked and re-probed with new primary antibodies. Preparation of the stripping solution is described in detail in Appendix 2: Solutions.

The same detection solution as mentioned above was used.

Table 3.4. Summary of antibody dilutions used in chemiluminescent detection

Primary antibody	**Dilution**	**Diluent**	**Secondary antibody**	**Dilution**	**Diluent**
Rabbit anti-Nrf2 antibody	1:1,000	Milk (3% (w/v)) solution	Goat anti-rabbit antibody	1:30,000	Milk (3% (w/v)) solution
Rabbit anti-HPRT antibody	1:3,000	Milk (3% (w/v)) solution			
Mouse anti-Lamin B1 antibody	1:1,000	Milk (3% (w/v)) solution	Goat anti-mouse antibody	1:5,000	Milk (3% (w/v)) solution
Mouse anti-GAPDH antibody	1:1,3000	BSA (3% (w/v)) solution[a]			BSA (3% (w/v)) solution

[a]: Preparation of BSA (3% (w/v)) solution is described in detail in Appendix 2: Solutions.

Fluorescent detection

All nuclear fraction (approximately 10 µL), 65 µL of whole cell and cytosolic fraction was used in gel electrophoresis. The bolt gel was run for 63 minutes at 140 V.

Detection of Nrf2, HPRT, GADPH and Lamin B1 was done simultaneously by using AzureSpectra rb650/ms550 western kit, with fluorescent block. The protocol supplied in the kit was followed. After SDS-PAGE, the proteins were blotted to a low fluorescence PVDF membrane. Later, the membrane was blocked for 1 hour at RT in 1x Azure fluorescent blot blocking buffer followed by 1-hour incubation at RT in primary antibodies. Antibody dilutions were the same as described above, but the solution used was 1x Azure fluorescent blot blocking buffer instead of milk (3% (w/v)) solution or BSA (3% (w/v)) solution. After the incubation, the membrane was washed with 1x Azure fluorescent blot washing solution (2 x 5 seconds and 3 x 5 minutes). Preparation of 1x Azure fluorescent blot washing solution is described in detail in Appendix 2: Solutions. Afterwards, the membrane was incubated for 1 hour at RT in secondary antibodies (1:2,500). The membrane was washed five times as described above followed by one wash of 5 minutes in TBS. After washing, the bands on the membrane were visualized. The settings for imaging Cy3 and Cy5 were used, producing a green and a red fluorescent color, respectively.

3.2.4 ELISA-based TransAM

Three experiments with different objectives were performed. The first experiment's purpose was to verify the quality of the positive control provided in the kit before it was used in detection. The second was performed to elucidate correlation between amount of nuclear fraction and Nrf2 level, while the third was performed to analyze and compare cytoplasmic levels of Nrf2 with levels in the nucleus.

Sample preparation

Samples and buffers were prepared according to the manufacturer's protocol. For cellular fraction, cell fractionation protocol (section 3.2.1.3) was used. The nuclear fractions were resuspended in complete lysis buffer, and agitated gently on ice for 30 minutes on an orbital shaker, and centrifuged at 14,000 x *g* for 10 minutes at 4 °C. The supernatant containing nuclear protein was collected.

Detection of Nrf2 level

Nrf2 level in cell fractions were detected using the ELISA-based TransAM according to the manufacturer's protocols. The competitive assay was performed only with the positive control provided in the kit because of the shortage of nuclear fraction material.

For blocking, complete binding buffer was added to each well. In wells with competitive assay, complete binding buffer containing either wild-type oligonucleotide or mutated oligonucleotide was added instead. The plate was sealed and incubated with mild agitation for 1 hour at RT. After incubation, each well was washed 3 times with 1x washing buffer. Then, anti-Nrf2 antibody (1:1,000) was added to each well. The plate was sealed and incubated for 1 hour at RT without agitation. After that, each well was washed 3 times. Subsequently, secondary antibody (1:1,000) was added followed by sealing and incubation without agitation as described above. After the incubation, each well was washed 4 times. To visualize the ARE-bound Nrf2/anti-Nrf2/secondary antibody complex, developing solution was added. The plate was incubated for 15 to 30 minutes at RT without agitation and protected from direct light. The development solution reacted with HRP, producing blue color. After the incubation, stop solution was added to cease the blue color development. The color turned from blue to yellow in the wells. Absorbance was measured at a wavelength of 450 nm (Ab450) and at a reference wavelength of 655 nm (Ab655) in the Synergy H1 microplate reader.

To determine the Nrf2 level, optical density at 450 nm ($OD_{450\ nm}$) or corrected absorbance values at 450 nm (corrected Ab450) were calculated by subtracting the Ab655 values from the Ab450 values. The $OD_{450\ nm}$ values expressed the Nrf2 level in the fraction samples.

3.2.5 Statistical analysis

Average (A), standard deviation (SD) and coefficient of variation (CV%) were calculated to compare the two methods utilized in isolation of PBMCs in blood samples.

In ELISA-based TransAM, Nrf2 levels, expressed as $OD_{450\ nm}$ values, in replicates of blank and of test samples were measured. Then, the average of $OD_{450\ nm}$ values of blank (A_{blank}), the average of $OD_{450\ nm}$ values of test samples (A), standard deviation of $OD_{450\ nm}$ values of blank (SD_{blank}) and standard deviation of $OD_{450\ nm}$ values of test samples (SD) were calculated.

Limit of blank (LOB) is the lowest concentration of analyte which exceeds zero. Limit of detection (LOD) is the lowermost concentration of analyte which exceeds LOB. The LOD of Nrf2 level was determined according to formula 2 and 3, where SD_{sample} was the SD of sample with lowest Nrf2 level:

$$LOD = LOB + 1.65 \times (SD_{sample}) \quad \text{(Formula 2) [96]}$$

$$LOB = A_{blank} + 1.65 \times (SD_{blank}) \quad \text{(Formula 3) [96]}$$

The results were assumed to approach normal distribution when the sample size increased. Student t-test was performed to determine whether Nrf2 levels in different samples measured in TransAM were significantly different from each other. A p value < 0.05 was considered significant.

4. Results

Samples and their labelling used in the experiments are presented in table 1 and table 2 in Appendix 1: Samples and their labelling.

4.1 Evaluation of isolation of PBMCs

Isolated cell samples from the same person, isolated with the two methods, varied from each other in PBMC count values and total protein concentration. Variation in PBMC count values were much larger than variation in total protein concentrations (table 4.1).

Table 4.1. PBMC count values (x 10^9/L) and total protein concentrations (mg/mL) in isolated cell samples. The number of blood samples from one person used in each method was three (n=3). A_1, SD_1 and CV_1: average, standard deviation and coefficient of variation, respectively, of PBMC count values. A_2, SD_2 and CV_2: average, standard deviation and coefficient of variation, respectively, of total protein concentrations.

A. Method 1

Sample	n	PBMC count values (x 10^9/L)			A_1	SD_1	CV_1 (%)	Total protein concentrations (mg/mL)			A_2	SD_2	CV_2 (%)
P1	3	94.1	55.2	144.4	97.9	44.7	45.7	2.6	2.2	2.4	2.4	0.2	7.6
P2	3	216.3	226.5	197.8	213.5	14.5	6.8	4.2	4.4	3.6	4.1	0.4	10.0
P3	3	250.2	636.0	377.8	421.3	196.5	46.6	7.8	3.9	6.8	6.2	2.1	33.3

B. Method 2

Sample	n	PBMC count values (x 10^9/L)			A_1	SD_1	CV_1 (%)	Total protein concentrations (mg/mL)			A_2	SD_2	CV_2 (%)
P1	3	23.4	71.5	61.0	52.0	25.3	48.7	1.1	1.1	0.9	1.0	0.1	12.5
P2	3	140.0	120.0	70.5	110.2	35.8	32.5	1.0	1.0	0.9	1.0	0.1	9.3
P3	3	223.9	100.1	124.7	149.6	65.5	43.8	0.9	0.8	1.2	0.9	0.2	21.9

The results showed that method 1 gave a higher yield of isolated cells than method 2. Protein concentration in cell samples isolated by method 1 was also higher than in cell samples isolated by method 2 (figure 4.1).

A.

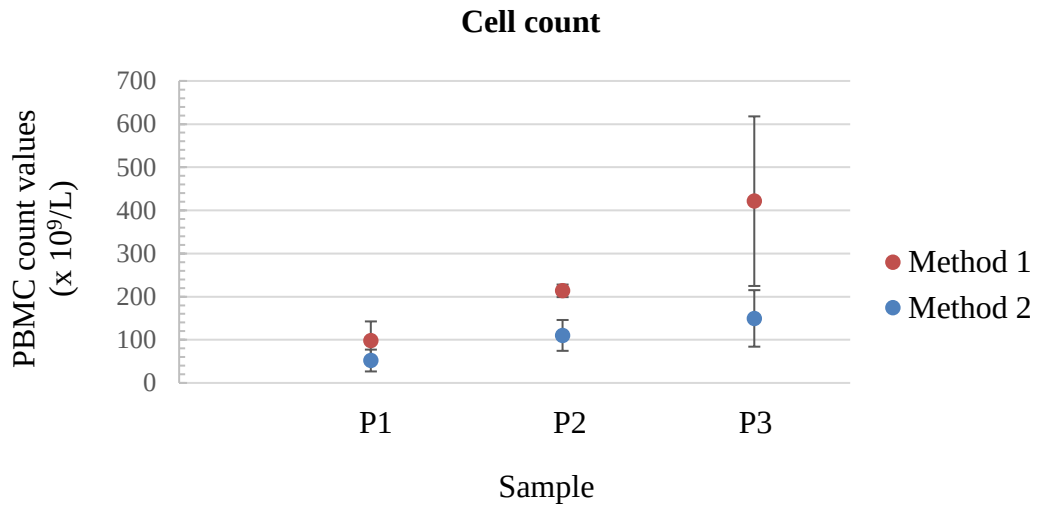

B.

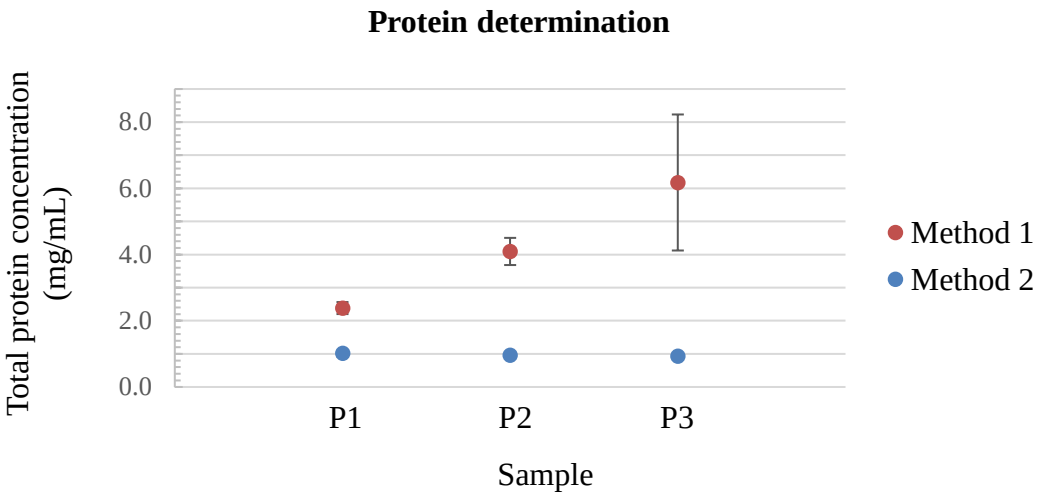

Figure 4.1. Six blood samples, each from three individuals, were isolated by method 1 (n=3) and method 2 (n=3), denoted by red and blue indicators, respectively. Error bars display the standard deviation values.

(A) Average of PBMC count values (x 10^9/L ± SD_1, n=3)

(B) Average of total protein concentrations (mg/mL ± SD_2, n=3)

4.2 Western blot

According to the manufacturers, anti-Nrf2 (C-term) from Cayman detect polyubiquitinated Nrf2 (pNrf2) at 90 kilodalton (kDa), anti-Nrf2 (N-term) from Cayman detects pNrf2 at 90 kDa and native Nrf2 (nNrf2) at 67 kDa, and anti-Nrf2 from Active Motif detect pNrf2 at 96 kDa.

4.2.1 Characterization of Nrf2 in lysed PBMCs

The MWs of detected bands in each lane in the triplicates or the quadruplicates were estimated in ImageJ [97]. The MWs of the detected bands in each lysate are mean values of MWs of each replicate.

Anti-Nrf2 (C-term) detected pNrf2 in the all three lysates, giving prominent protein bands whose MWs ranging from approximately 94 to 96 kDa. Nrf2 bands were marked in bold font (figure 4.2).

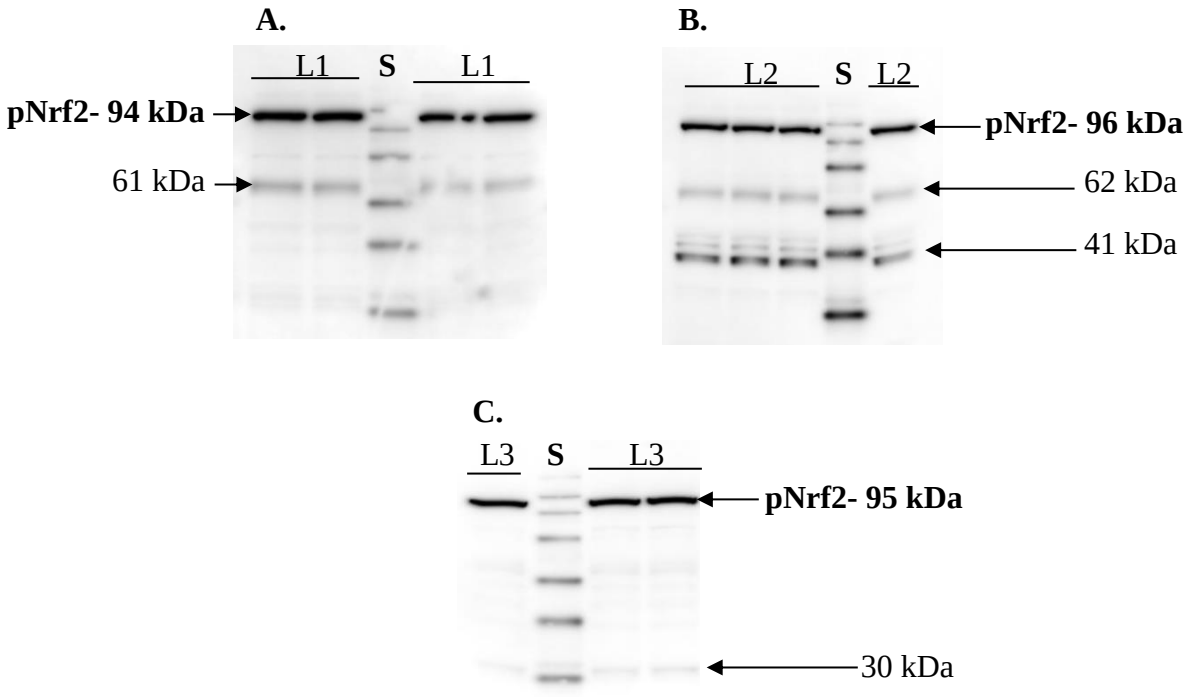

Figure 4.2. Representative images of different blots after Western blot analysis of the three lysate samples: L1 (A), L2 (B) and L3 (C) using the anti-Nrf2 (C-term) show one distinct band of the detected polyubiquitinated Nrf2 (pNrf2). Arrows indicate the positions at which the detected bands migrated. S: supersignal molecular weight protein ladder.

Anti-Nrf2 (N-term) antibody detected both pNrf2 and nNrf2 in the three lysates, marked in bold font (figure 4.3). Bands of pNrf2 migrated at apparent MW of 94 kDa in lysate 1 and 95 kDa in lysate 2 and 3, while nNrf2 bands migrated at MW of 71 kDa in lysate 1 and 3 and 72 kDa in lysate 2.

Using anti-Nrf2 antibody from Active Motif (AM), multiple bands with different MWs emerged. Many of them were faint. One band in lysate 2 (L2) at about 94 kDa might be pNrf2 (figure 4.4). No pNrf2 detected in lysate 1 and 3.

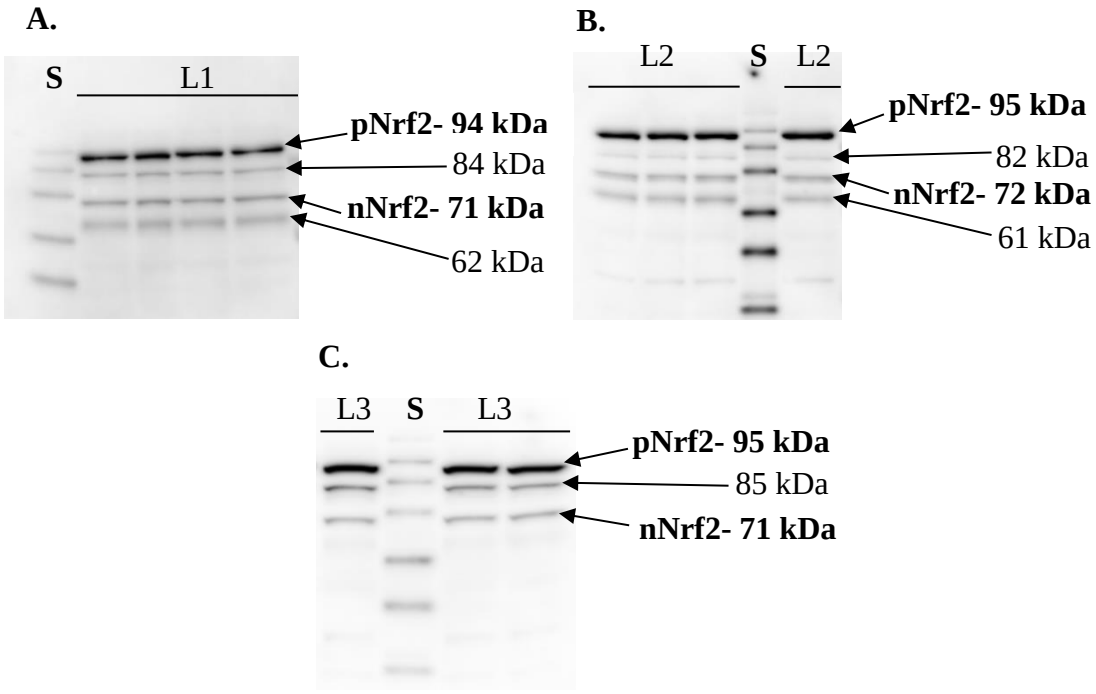

Figure 4.3. Anti-Nrf2 (N-term) detected polyubiquitinated Nrf2 (pNrf2) and native (nNrf2) in all three lysates: L1 (A), L2 (B) and L3 (C). Arrows indicate the positions at which the detected bands migrated. S: supersignal molecular weight protein ladder.

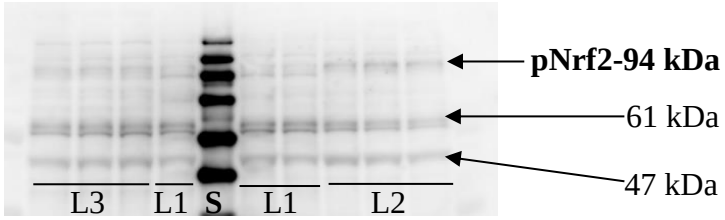

Figure 4.4. Representative image of Western blots after detection of polyubiquitinated Nrf2 (pNrf2) in the three lysate samples (L1, L2 and L3) using the anti-Nrf2 antibody from AM. Arrow indicates the location of Nrf2 band. S: supersignal molecular weight protein ladder.

Secondary antibody control

Without primary antibody, the secondary antibody detected bands at 53 kDa, 87 kDa and 120 kDa (figure 4.5).

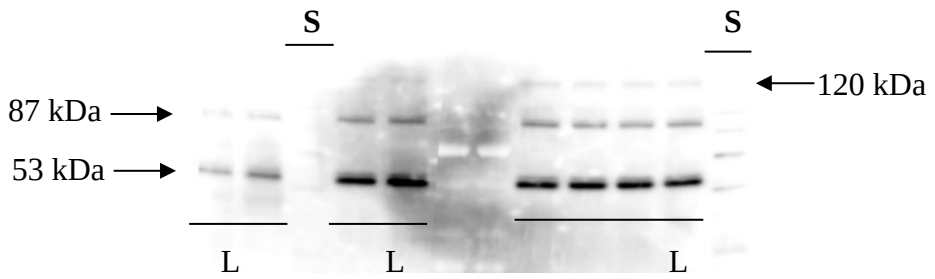

Figure 4.5. In the absence of the primary antibody, the secondary antibody detected nonspecific bands at 53 kDa, 87 kDa and 120 kDa on the blot. L: Lysate. S: supersignal molecular weight protein ladder.

4.2.2 Nrf2 detection in cellular fractions and purity determination

The predicted molecular weights of HPRT, GAPDH and Lamin B1, supplied by the manufactures, are 25 kDa, 36 kDa and 68 kDa, respectively.

The shown MW of detected protein in one sample was the mean value of three different MWs of the same protein detected in each fraction from this sample. To quantify obtained band, the band intensity was determined. Band intensity was proportional to the amount of the protein detected. The brighter the band, the higher the band intensity value. Both band intensities and MWs were determined using ImageJ [97].

Chemiluminescent detection

Anti-Nrf2 (N-term) antibody detected both pNrf2 and nNrf2 in the whole cell, cytosolic and nuclear fractions, but pNrf2 was the dominant form in all fractions compared with nNrf2. No nNrf2 was detected in three of the nuclear samples (N4, N5 and N6). In the cytosolic fractions, levels of pNrf2 and nNrf2 were much higher than those of pNrf2 and nNrf2 in the nuclear fractions (table 4.2). Reference proteins HPRT, GAPDH and Lamin B1 were detected in all fractions, but the amounts were varying from fractions to fractions (figure 4.6 and 4.7).

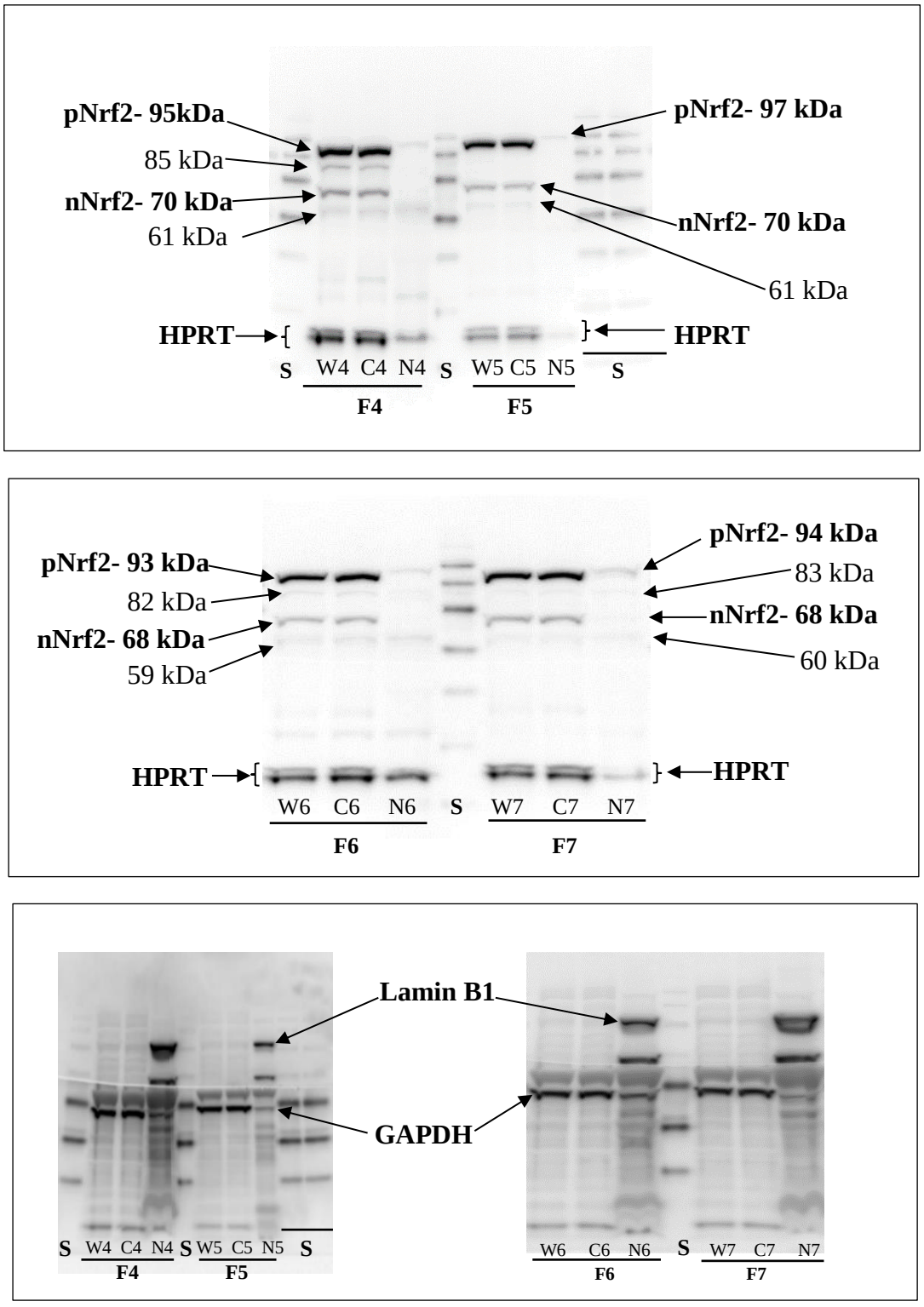

Figure 4.6. Representative images of Western blots for polyubiquitinated Nrf2 (pNrf2), native Nrf2 (nNrf2), HPRT, Lamin B1 and GAPDH detected in the fractions from F4, F5, F6 and F7. Arrows indicate the positions at which the detected bands migrated. S: supersignal molecular weight protein ladder. W: whole cell fraction. C: cytosolic fraction. N: nuclear fraction.

GAPDH and HPRT were strongly detected in whole cell and cytosolic fractions. Small amounts of HPRT and GAPDH were also present in nuclear fractions. The amount of Lamin B1, on the other hand, was high in the nuclear fractions and low in the whole cell and cytosolic fractions. Whole cell and cytosolic fractions contained almost equal amounts of pNrf2 (figure 4.7).

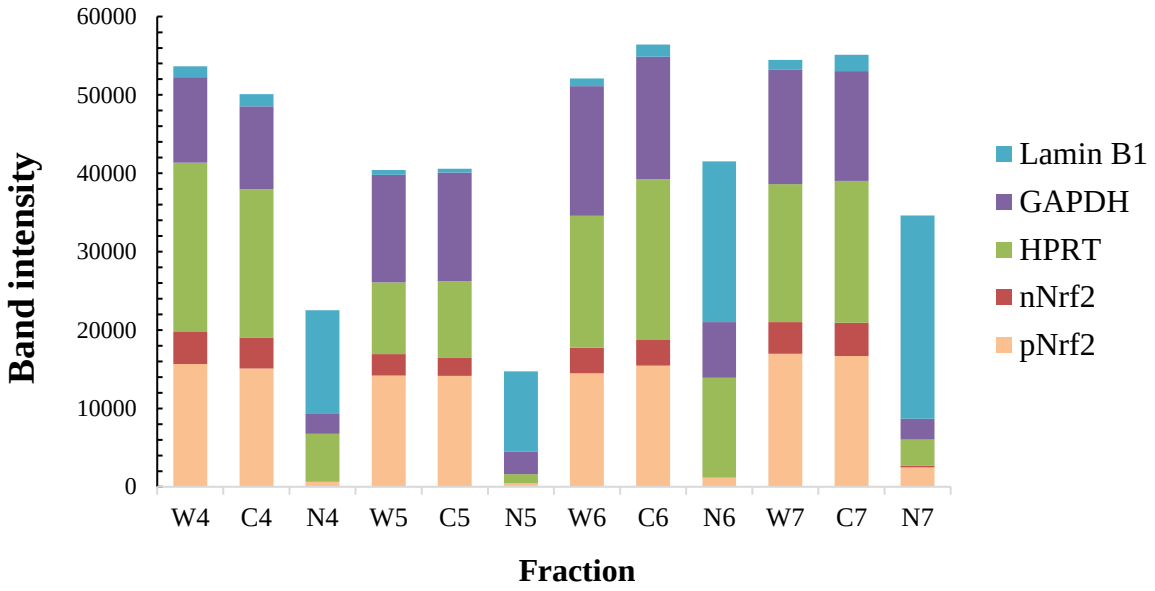

Figure 4.7. Relative quantifying of the proteins which were detected in the different cellular fractions. W: whole cell fraction. C: cytosolic fraction. N: nuclear fraction.

Table 4.2. Ratios between cytosolic pNrf2 level and nuclear pNrf2 level and between cytosolic nNrf2 level and nuclear nNrf2 level. C: cytosolic fraction. N: nuclear fraction

Fraction	**Band intensities**		**pNrf2 ratio**	**nNrf2 ration**
	pNrf2	nNrf2	**(C_{pNrf2}/N_{pNrf2})**	**(C_{nNrf2}/N_{nNrf2})**
C4	15080	3967	24.5	-
N4	616	0		
C5	14159	2300	32.3	-
N5	439	0		
C6	15449	3280	13.1	-
N6	1178	0		
C7	16695	4257	6.7	18.8
N7	2482	227		

Fluorescent detection

Lamin B1 was detected only in the nuclear fractions, whereas GAPDH and HPRT were strongly detected in all whole cell and cytosolic fractions. The levels of cytosolic pNrf2 and nuclear pNrf2 were higher than the levels of nuclear pNrf2 and nNrf2 in all fractions except fractions C10 and N10. Fraction C10 contained less nNrf2 than fraction N10. In addition, no pNrf2 was detected in fraction N10. Beyond that, both pNrf2 and nNrf2 were detected in the other nuclear fractions and all whole cell and cytosolic fractions (table 4.3). Notably, a faint band of GAPDH was observed in all nuclear fractions, whereas a faint band of HPRT was observed in nuclear fraction N10 (figure 4.8).

Table 4.3. Levels of pNrf2 and nNrf2 in the cellular fractions expressed as band intensities. Ratios between levels of cytosolic pNrf2 and nuclear pNrf2 and between levels of cytosolic nNrf2 and nuclear nNrf2 are also presented. W: whole cell fraction. C: cytosolic fraction. N: nuclear fraction

Fractions	**Band intensities**		**pNrf2 ratio (C/N)**	**nNrf2 ratio (C/N)**
	pNrf2	nNrf2		
W8	8912	2024		
C8	8081	1685	90.9	1.5
N8	89	1120		
W9	11808	1068		
C9	14292	1723	28.4	1.2
N9	504	1445		
W10	14225	2702		
C10	13382	2427	-	0.6
N10	0	4258		
W11	15739	3483		
C11	15482	4421	9.2	1.2
N11	1690	3617		

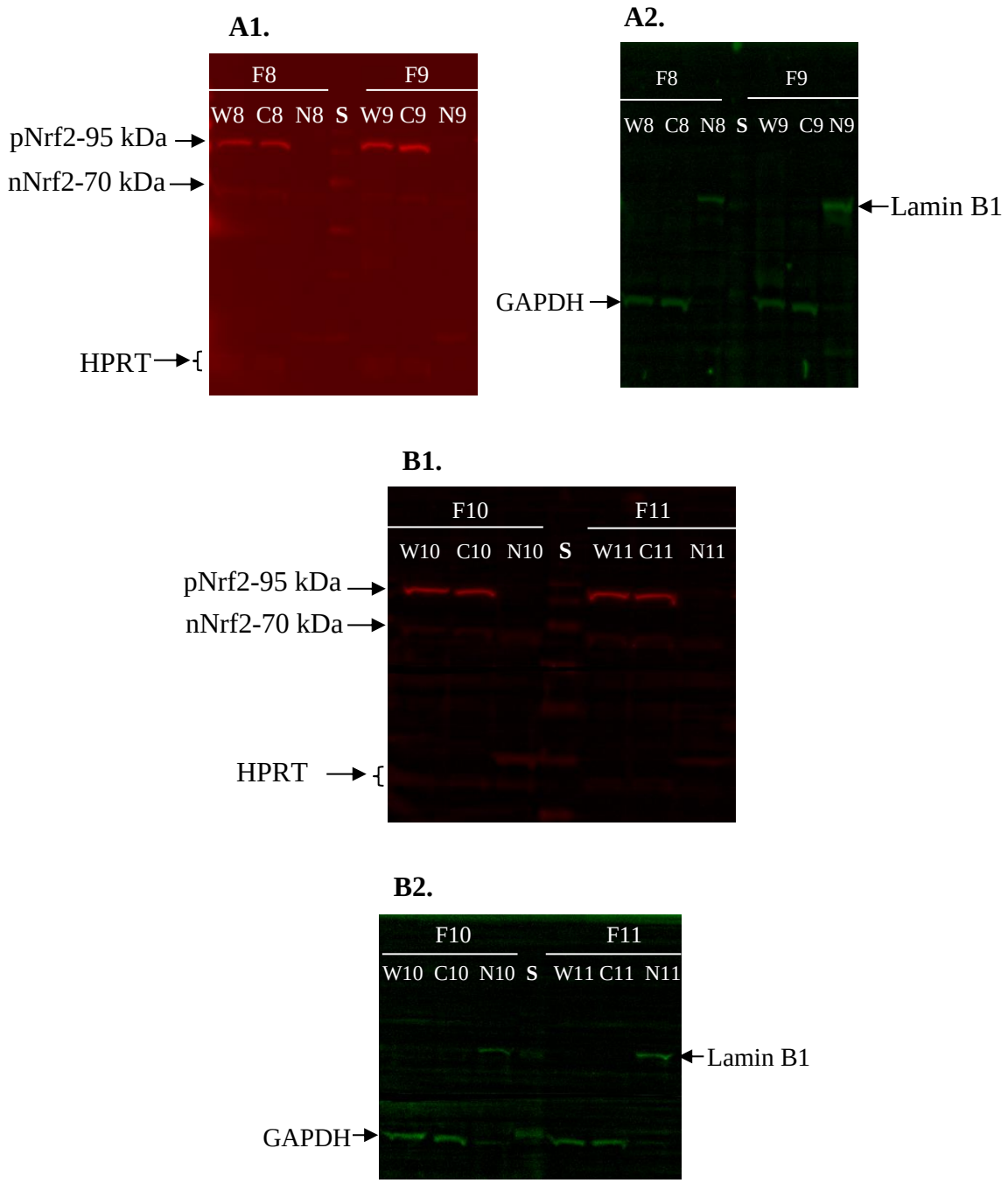

Figure 4.8. Singel-channel scanned images of blots from the multiplexed fluorescent detection of Nrf2, HPRT, Lamin B1 and GAPDH in the cellular fractions. Nrf2 and HPRT, labelled with Cy5 conjugated to goat anti-rabbit, were detected in the red channel, while Lamin B1 and GAPDH, labelled with Cy3 conjugated to goat anti-mouse, were detected in the green channel accordingly. Arrows indicate the positions of signals from the detected proteins. S: supersignal molecular weight protein ladder. W: whole cell fraction. C: cytosolic fraction. N: nuclear fraction. A1 and A2 is the same membrane, and so is B1 and B2.

4.3 ELISA-based TransAM

Verification of ELISA kit

The results from the experiment are reported in table 4.4. LOD ($OD_{450\ nm}$) in the experiment is $0.01155 \approx 0.012$ (formula 2).

Table 4.4. Nrf2 level in different controls expressed as optical density at 450 nm ($OD_{450\ nm}$)

Sample	**n**	**$OD_{450\ nm}$**		
		A	SD	CV (%)
Blank	8	0.000	0.004	-
P[a]	8	0.081	0.011	14.166
PW[b]	4	0.058	0.003	4.473
PM[c]	4	0.093	0.003	3.649

A: average. SD: standard deviation. CV: coefficient of variation.

[a]: Positive control with no competitive element.

[b]: Positive control with competitive wild-type consensus oligonucleotide.

[c]: Positive control with non-competitive mutated consensus oligonucleotide.

The average Nr2 level in wells with only positive control (P) and wells with positive control and non-competitive mutated oligonucleotide (PM) was significantly higher than the average Nrf2 level in wells with positive control and wild-type competitor (PW) ($p < 0.05$). There was no significant difference ($p > 0.05$) between the wells with only P and the wells with PM although the former had a lower average Nrf2 level than the latter, 0.081 and 0.093, respectively (figure 4.9). The results were as expected. The kit was therefore verified.

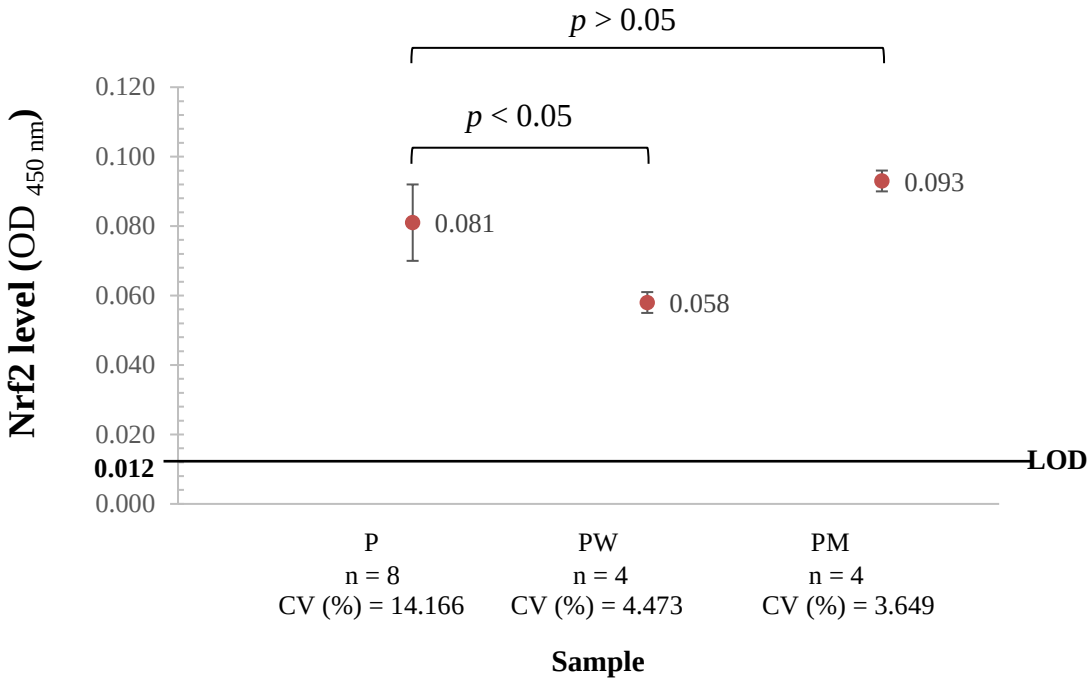

Figure 4.9. Average of Nrf2 levels (± SD) in wells with positive control (P), in wells with positive control and the competitive wild-type oligonucleotide (PW) and in wells with positive control and the non-competitive mutated oligonucleotide (PM). $OD_{450\ nm}$: optical density at 450 nm.

Nrf2 level in nuclear fractions

The average Nrf2 level in N13a was higher than the average Nrf2 level in N13b, which was as expected because N13a had a higher amount of nuclear fraction than N13b. By contrast, the average Nrf2 level in the nuclear fraction N12a was lower than the average Nrf2 level in the nuclear fraction N12b although the former sample contained twofold more nuclear material than the latter (table 4.5). LOD ($OD_{450\ nm}$) in the experiment is $0.0198 \approx 0.020$ (formula 2). In six of eight nuclear functions, the average Nrf2 levels fell below the LOD. In sample N13a and N14a, the error bars reached 0, while in sample N14b, N15a and N15b, the error bars reached the negative side of the y-axis. This indicated that those samples might not contain Nrf2 (figure 4.10).

Table 4.5. Average Nrf2 level expressed as optical density at 450 nm ($OD_{450\ nm}$) in controls and in samples with different amount of nuclear fraction.

Sample	n	OD 450 nm		
		A	SD	CV (%)
Blank	4	0.000	0.004	-
P[a]	4	0.058	0.005	8.963
PW[b]	4	0.050	0.019	38.046
PM[c]	4	0.067	0.011	15.847
N12a	5	0.012	0.003	27.812
N12b	5	0.024	0.005	20.581
N13a	5	0.028	0.004	13.314
N13b	5	0.008	0.008	106.665
N14a	5	0.006	0.006	101.389
N14b	5	0.004	0.009	192.891
N15a	5	0.000	0.008	38764.352
N15b	5	0.003	0.005	161.018

A: average. SD: standard deviation. CV: coefficient of variation.

[a]: Positive control with no competitive element.

[b]: Positive control with competitive wild-type consensus oligonucleotide.

[c]: Positive control with non-competitive mutated consensus oligonucleotide.

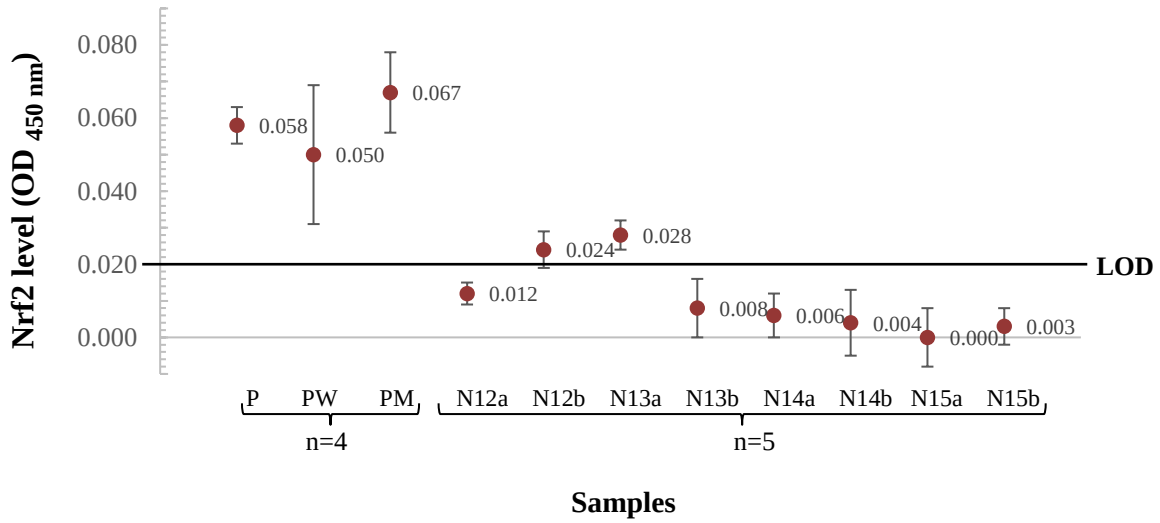

Figure 4.10. Average Nrf2 level (± SD) in controls and in the nuclear fractions. $OD_{450\ nm}$: optical density at 450 nm. P: positive control and no competitive element. PW: positive control and competitive wild-type consensus oligonucleotide. PM: positive control and non-competitive mutated consensus oligonucleotide.

Nrf2 in cytosolic and nuclear fractions

LOD (OD $_{450\ nm}$) in the experiment is 0.01818 ≈ 0.018 (formula 2). In three of four nuclear functions, the average Nrf2 levels fell below the LOD. On the contrary, the average Nrf2 levels in all four cytosolic fractions exceeded the LOD (table 4.6 and figure 4.11). Moreover, the cytosolic fractions contained significantly higher average Nrf2 level than the nuclear fractions ($p < 0.05$) (table 4.6 and figure 4.12).

Table 4.6.

A. Average Nrf2 level expressed as optical density at 450 nm (OD $_{450\ nm}$) in controls, cytosolic fractions and nuclear fractions.

B. Calculated average of Nrf2 levels of all four cytosolic and nuclear fractions

A.

Sample	n	**OD $_{450\ nm}$**		
		A	SD	CV (%)
Blank	4	0	0.007	-
P[a]	4	0.095	0.012	12.635
PW[b]	4	0.038	0.008	21.133
PM[c]	4	0.073	0.011	14.906
C16	3	0.047	0.005	10.427
N16	3	0.002	0.004	203.191
C17	3	0.039	0.003	7.614
N17	3	0.021	0.002	9.323
C18	3	0.035	0.002	6.635
N18	3	0.010	0.007	63.705
C19	3	0.053	0.011	20.408
N19	3	0.017	0.008	47.234

B.

Sample	n	**A (OD $_{450\ nm}$)**	
		Cytosolic fractions	**Nuclear fractions**
16	3	0.047	0.002
17	3	0.039	0.021
18	3	0.035	0.010
19	3	0.053	0.017
A $_{Nrf2\ level\ in\ all\ fractions}$		0.044	0.013
SD $_{Nrf2\ level\ of\ all\ fractions}$		0.007	0.007

A: Average. SD: standard deviation. CV: coefficient of variation.

[a]: Positive control with no competitive element.

[b]: Positive control with competitive wild-type consensus oligonucleotide.

[c]: Positive control with non-competitive mutated consensus oligonucleotide.

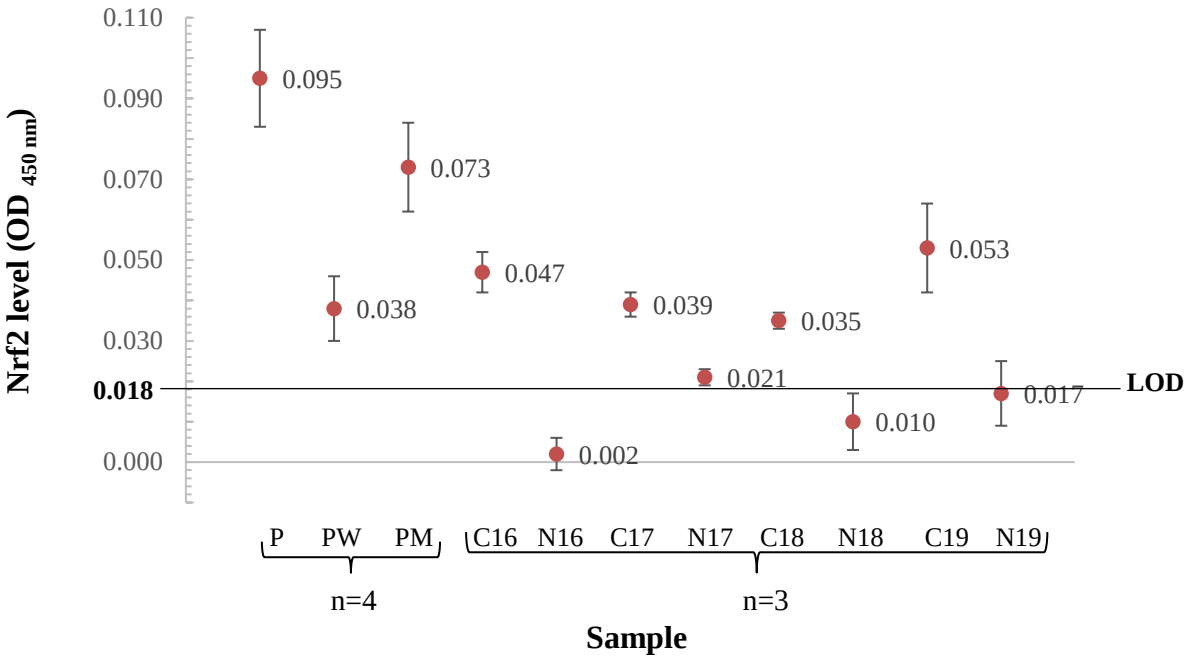

Figure 4.11. Average Nrf2 level (± SD) in controls, cytosolic and nuclear fractions from four healthy people. LOD=0.021. $OD_{450\ nm}$: optical density at 450 nm. P: positive control and no competitive element. PW: positive control and competitive wild-type consensus oligonucleotide. PM: positive control and non-competitive mutated consensus oligonucleotide.

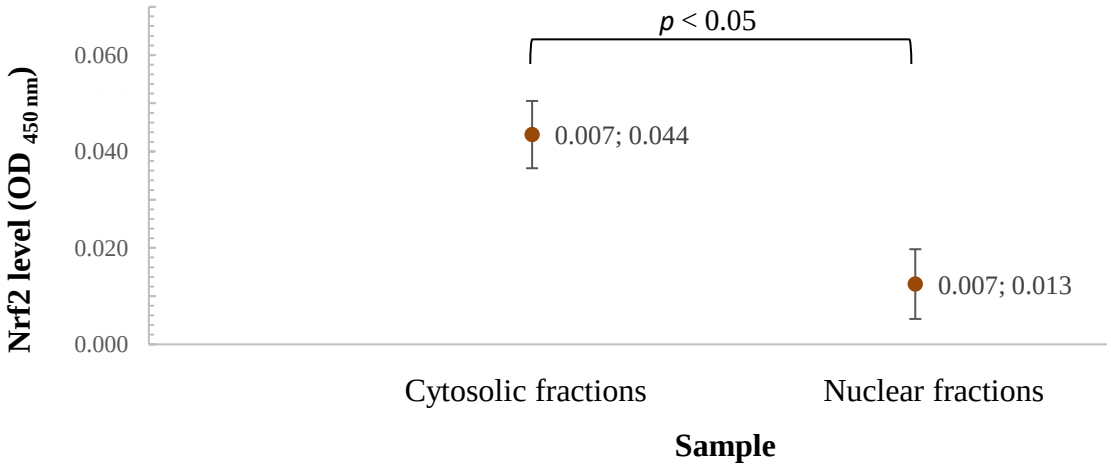

Figure 4.12. Two-tailed Student's *t*-test for paired values was performed for comparison of the average Nrf2 levels between the cytosolic and nuclear fractions (n=3, $p < 0.05$).

5. Discussion

5.1 Evaluation of isolation of PBMCs

The numbers of PBMCs in samples isolated by method 2 were not as high as the numbers of PBMCs in samples isolated by method 1. As a result, the protein concentrations in those samples were also low compared to the protein concentrations in the samples with PBMCs isolated by the first method. The main reasons for the differences might be the short centrifugation time, which was 10 minutes, and the low centrifugation speed, which was 200 x *g*, applied in method 2. Therefore, even though method 1 showed a greater dispersion of cell count and total protein values, i.e. higher CV, than the other did, the results proposed that method 1 was better than method 2 in isolating PBMCs in blood samples.

When analyzing blood samples taken from the same person, it is expected that the values of cell counting performed on these samples will not be significantly different. The results, on the other hand, demonstrated a significant difference in the numbers of PBMCs regardless of isolation method used. This was explained in the high SD and CV of both methods (table 4.1). The values of SD and CV indicated that both methods produced almost the same high dispersion of PBMC count numbers. It may be due to factors disturbing the measurement; the first could be aggregation of mononuclear cells because they were up-concentrated in small volume, and the second could be cell loss during isolation.

However, the determination of protein concentration in isolated cell samples gave converse results. The calculated values of SD and CV were small regardless of isolation method. When CV from protein concentration determination was compared with CV from cell counting, it was quite evident that protein concentration was a better implement to evaluate isolation yield.

5.2. Western blot

5.2.1 Nrf2 in lysates and cellular fractions

Nrf2 was successfully detected in all lysates of PBMCs, indicating a considerable expression of the protein in PBMCs. Furthermore, the detection provided evidence to support the case that pNrf2 is more abundant than nNrf2 in the PBMCs (figure 4.2 and 4.3). This was

plausible as it is well established that Keap1 constantly promotes Nrf2 ubiquitination and subsequent proteasomal degradation under homeostatic conditions. This regulatory pathway was also verified in WBCs in the study of Murakami et al. (2014) [98]. Although the MWs of detected Nrf2 were not identical to the MWs provided by the manufacturers, the differences between them were not significant. Moreover, Lau et al. have proved that Nrf2 migrates between approximately 95-110 kDa [99] despite its theoretical MW of about 68 kDa [100]. The discrepancy may be due to the abundance of acid residues in Nrf2 [99, 101] and the interaction between Nrf2 and actin [102]. Moreover, post-translational modification of Nrf2 *in vivo* including acetylation, ubiquitination and phosphorylation [17, 45] could lead to slower mobility [103-105]. As ubiquitin has a MW of about 9 kDa [106], polyubiquitinated Nrf2 could typically migrate a minimum 9 kDa slower than its unmodified forms, giving bands with higher MW then the theoretical MW.

The characterization of Nrf2 in lysates showed that unstressed PBMCs contained a higher level of pNrf2 than nNrf2. The results of Nrf2 detection in cellular fractions of PBMCs and band intensities suggested the same conclusion (figure 4.6). They illustrated, at the same time, two points. First, whole cell and cytosolic fractions from the same person had almost equal level of Nrf2, and their overall Nrf2 level was higher than overall Nrf2 level in the nuclear fractions (figure 4.6 and 4.7). Second, in both cytosolic and nuclear fractions, the level of pNrf2 was higher than the level of nNrf2 (table 4.2). In addition, when anti-Nrf2 (N-term) antibody was used, the migration pattern of Nrf2 in chemiluminescent detection in whole cell and cytosolic fractions was identical to that of Nrf2 in lysates. The bands were also detected at similar MWs as those in the lysates. By closer inspection of the images of the blots, the same pattern can also be observed in lanes loaded with nuclear fractions N6 and N7 although the bands are very faint (figure 4.3 and 4.6).

The results from fluorescent detection supported the findings in chemiluminescent detection. In whole cell and cytoplasm, the overall Nrf2 level in whole cell and cytosolic fractions was higher than the overall Nrf2 level in the nuclear fraction, and the amounts of cytosolic pNrf2 and nNrf2 were generally higher than the amounts of nuclear pNrf2 and nNrf2 (table 4.3 and figure 4.8).

The Nrf2 activity in cells is tightly regulated by diverse pathways. Some of them have been identified, while some remain elusive [17]. For this reason, some observed bands on the membranes of the lysates and the fractions could be a form of Nrf2. The size of Nrf2 can be reduced by proteolysis as protease inhibitor was not used in RIPA buffer or by post-translation cleavage. Ohtsubo et al. (1999) identified Nrf2 as a substrate for capase-3 *in vivo*

and *in vitro*. Caspases are cysteine proteases which are central molecule in inflammasomes, and thus play an essential role in apoptosis, an active form of cell death. In the study, Nrf2 was cleaved and inactivated by caspase-3, producing two C-terminal fragments, 50 kDa and 30 kDa [107]. Therefore, bands detected by anti-Nrf2 (C-term) at approximately 30 kDa or 50 kDa might be caspase-cleaved forms of Nrf2. However, the interaction between caspase Nrf2 is not fully understood as it has been very limited investigated so far. Several groups have additionally demonstrated that Nrf2 is ubiquitinated and subsequently proteasomally degraded not only in cytoplasm but also in the nucleus [102, 108, 109]. Their finding substantiates the appearance of pNrf2 bands in the nuclear fractions and support the speculation that multiple bands detected in the nucleus might also be other forms of Nrf2. On the other hand, the equivocal bands may rather be non-specific. The secondary antibody control revealed that the anti-rabbit IgG HRP-conjugated secondary antibody could produce nonspecific bands (section 4.2.1).

To confirm the equivocal bands were indeed Nrf2, cells should have been treated with canonical Nrf2 inducers such as tert-butylhydroquinone (tBHQ) or sulforaphane (SFN). Bands belonging to Nrf2 would increase in intensity in response to the treatment [99, 105]. Another way to identify specific bands would be to cut out bands from the gel and extract proteins from these bands. Specific proteins in the bands could then be identified using mass spectrometry [110].

5.2.2 Purity determination

The results from chemiluminescent detection were in concordance with the results from fluorescent detections. Nuclear lamina found inside the nucleus was present in the nuclear fractions as Lamin B1 which was strongly detected. In the whole cell and cytosolic fractions, HPRT and GAPDH were the dominant proteins (figure 4.6, 4.7 and figure 4.8). The essence of the fractions was confirmed.

Results from Western blot indicated that fractionation of PBMCs in blood samples using REAP protocol was able to provide relatively pure fractions. Further test experiments are therefore required to modify the method to obtain more pure fractions. It is worth noting that although fractionation has widely been used in most researches where cells are involved, it is difficult to find reports in which fractions from WBCs are mentioned. The reason may be that WBCs are among the smallest cells in the body [18, 84], making fractionation difficult.

Compounding the limitation is the fact that number of isolated cells after isolation is low unless more than one blood sample is used. This issue raises questions about how many blood samples and how much PBMCs are needed to obtain sufficient fraction material.

5.3 ELISA-based TransAM

In attempt to increase detected Nrf2 levels, two nuclear samples were merged to one. However, the correlation between amount of nuclear fraction used and Nrf2 level failed to be established because the results were generally scattered. One reason may be that it was difficult to make exact replicates of nuclear fractions because of very limited numbers of isolated cells available; another may be that TransAM might be not sufficiently sensitive to detect Nrf2 level below LOD. As a result, some CVs were high, and some error bars reached the negative side (table 4.5 and figure 4.10). The first reason may be more rational as Nrf2 expression level is supposed to be higher in granulocytes, monocytes and hematopoietic stem and progenitor cells (HSPCs) [98].

In the third experiment, the cytosolic fractions exhibited significantly higher Nrf2 levels than the nuclear fraction, which corresponded to the observations in the Western blot detection. The results of this experiment were consistent, suggesting that TransAM was more appropriate for Nrf2 measurement in cells with high Nrf2 abundance.

5.4 Strengths and limitations of the study

There were some shortcomings in the analyses. Protein concentration determination in the cellular fractions prior to gel electrophoresis, and purity determination before TransAM assay were not performed because of the shortage of nuclear material. In addition, the sample size for TransAM assay was small, and all samples were solely from healthy individuals. Moreover, the two methods themselves have both advantages and disadvantages. Western blot provided more dimensions for studying Nrf2 in PBMCs than TransAM assay. In Western blot, Nrf2 migration pattern and different forms of Nrf2 were uncovered. In addition, MW of Nrf2 and its level were determined. The disadvantage was that there is still confusion regarding the correct MW of Nrf2 detected and the specificity of anti-Nrf2 antibodies. TransAM assay was a more time-saving implement compared to Western blot for detection

and quantifying Nrf2. However, it might have difficulty in detecting and quantifying low amounts of Nrf2.

6. Conclusions

PBMCs were revealed to contain both pNrf2 and nNrf2 with a distinct migration pattern in Western blot. The level of pNrf2 appeared to be higher than the level of nNrf2 in these cells. The results from both Western blot and TransAM assay showed, at the same time, that most Nrf2 was contained in the whole cell and cytosolic fraction as a very low level of nuclear Nrf2 was detected.

In addition, this study demonstrated that both Western blot and TransAM were able to detect Nrf2 and measure Nrf2 level in cellular fractions of PBMCs. Whether Nrf2 can be used as a supplementary biomarker to evaluate oxidative stress-induced antioxidant status remains to be determined. Additional experiments are required to:

- obtain more pure fractions of PBMCs that can be used in TransAM assay. Their purity can be verified, if desired, in Western blot.
- evaluate if TransAM is suitable for measurement of Nrf2 level in fractions from PBMCs, and if it can provide reliable results when the sample size is increased.

7. References

[1] Halliwell, B. (2006) Reactive Species and Antioxidants. Redox Biology Is a Fundamental Theme of Aerobic Life, *Plant Physiology 141*, 312-322.

[2] Norheim, K. B., Jonsson, G., Harboe, E., Hanasand, M., Gøransson, L., and Omdal, R. (2012) Oxidative stress, as measured by protein oxidation, is increased in primary Sjøgren's syndrome, *Free Radical Research 46*, 141-146.

[3] Brieger, K., Schiavone, S., Miller, F. J., Jr., and Krause, K. H. (2012) Reactive oxygen species: from health to disease, *Swiss Medical Weekly 142*, w13659.

[4] Singh, M., and Moniri, N. H. (2012) Reactive oxygen species are required for β2 adrenergic receptor–β-arrestin interactions and signaling to ERK1/2, *Biochemical Pharmacology 84*, 661-669.

[5] Birben, E., Sahiner, U. M., Sackesen, C., Erzurum, S., and Kalayci, O. (2012) Oxidative Stress and Antioxidant Defense, *The World Allergy Organization journal 5*, 9-19.

[6] Halliwell, B. (2007) Biochemistry of oxidative stress, *Biochemical Society Transactions 35*, 1147-1150.

[7] Dalle-Donne, I., Rossi, R., Colombo, R., Giustarini, D., and Milzani, A. (2006) Biomarkers of oxidative damage in human disease, *Clinical Chemistry 52*, 601-623.

[8] Rahman, K. (2007) Studies on free radicals, antioxidants, and co-factors, *Clinical Interventions in Aging 2*, 219-236.

[9] Onorato, J. M., Thorpe, S. R., and Baynes, J. W. (1998) Immunohistochemical and ELISA assays for biomarkers of oxidative stress in aging and disease, *Annals of the New York Academy of Sciences 854*, 277-290.

[10] Halliwell, B., and Whiteman, M. (2004) Measuring reactive species and oxidative damage in vivo and in cell culture: how should you do it and what do the results mean?, *British Journal of Pharmacology 142*, 231-255.

[11] Tarpey, M. M., Wink, D. A., and Grisham, M. B. (2004) Methods for detection of reactive metabolites of oxygen and nitrogen: in vitro and in vivo considerations, *American Journal of Physiology: Regulatory, Integrative and Comparative Physiology 286*, R431-444.

[12] Ho, E., Karimi Galougahi, K., Liu, C. C., Bhindi, R., and Figtree, G. A. (2013) Biological markers of oxidative stress: Applications to cardiovascular research and practice, *Redox Biololgy 1*, 483-491.

[13] Tariq, A., Mansoor, M. A., Marti, H. P., Jonsson, G., Slettan, A., Weeraman, P., and Apeland, T. (2018) Systemic redox biomarkers and their relationship to prognostic risk markers in autosomal dominant polycystic kidney disease and IgA nephropathy, *Clinical Biochemistry 56*, 33-40.

[14] Surowiec, I., Gjesdal, C. G., Jonsson, G., Norheim, K. B., Lundstedt, T., Trygg, J., and Omdal, R. J. R. I. (2016) Metabolomics study of fatigue in patients with rheumatoid arthritis naïve to biological treatment, *Rheumatology International 36*, 703-711.

[15] Moi, P., Chan, K., Asunis, I., Cao, A., and Kan, Y. W. (1994) Isolation of NF-E2-related factor 2 (Nrf2), a NF-E2-like basic leucine zipper transcriptional activator that binds to the tandem NF-E2/AP1 repeat of the beta-globin locus control region, *Proceedings of the National Academy of Sciences of the United States of America 91*, 9926-9930.

[16] Taguchi, K., Motohashi, H., and Yamamoto, M. (2011) Molecular mechanisms of the Keap1-Nrf2 pathway in stress response and cancer evolution, *Genes to Cells 16*, 123-140.

[17] Farooqui, T., and Farooqui, A. A. (2012) *Oxidative stress in vertebrates and invertebrates : molecular aspects of cell signaling*, 1. ed., Wiley-Blackwell, Hoboken, New Jersey.

[18] Campbell, N. A., Reece, J. B., Urry, L. A., Cain, M. L., Waaserman, S. A., Minorsky, P. V., and Jackson, R. B. (2008) *Biology*, 8. ed., Pearson/Benjamin Cummings, San Francisco, California.

[19] Berg, J. M., Tymoczko, J. L., Stryer, L., and Gatto, G. J. (2012) *Biochemistry*, 7. ed., Freeman and Company, New York.

[20] Elliott, W. H., and Elliott, D. C. (2009) *Biochemistry and molecular biology*, 4. ed., Oxford University Press, Oxford.

[21] Sies, H. (1997) Oxidative stress: oxidants and antioxidants, *Experimental Physiology 82*, 291-295.

[22] Powers, S. K., Ji, L. L., Kavazis, A. N., and Jackson, M. J. (2011) Reactive oxygen species: impact on skeletal muscle, *Comprehensive Physiology 1*, 941-969.

[23] Chance, B., Sies, H., and Boveris, A. (1979) Hydroperoxide metabolism in mammalian organs, *Physiological Reviews 59*, 527-605.

[24] Valko, M., Leibfritz, D., Moncol, J., Cronin, M. T., Mazur, M., and Telser, J. (2007) Free radicals and antioxidants in normal physiological functions and human disease, *International Journal of Biochemistry and Cell Biology 39*, 44-84.

[25] Droge, W. (2002) Free radicals in the physiological control of cell function, *Physiological Reviews 82*, 47-95.

[26] Giorgio, M., Trinei, M., Migliaccio, E., and Pelicci, P. G. (2007) Hydrogen peroxide: a metabolic by-product or a common mediator of ageing signals?, *Nature Reviews: Molecular Cell Biology 8*, 722-728.

[27] Starkov, A. A. (2008) The Role of Mitochondria in Reactive Oxygen Species Metabolism and Signaling, *Annals of the New York Academy of Sciences 1147*, 37-52.

[28] Davies, M. J. (2005) The oxidative environment and protein damage, *Biochimica et biophysica acta (BBA)-Proteins and proteomics 1703*, 93-109.

[29] Halliwell, B. (2006) Oxidative stress and neurodegeneration: where are we now?, *Journal of Neurochemistry 97*, 1634-1658.

[30] Church, D. F., and Pryor, W. A. (1985) Free-radical chemistry of cigarette smoke and its toxicological implications, *Environmental Health Perspectives 64*, 111-126.

[31] Ma, Q. (2010) Transcriptional responses to oxidative stress: pathological and toxicological implications, *Pharmacology & Therapeutics 125*, 376-393.

[32] Niki, E. (2014) Antioxidants: Basic principles, emerging concepts, and problems, *Biomedical Journal 37*, 106-111.

[33] Ma, Q. (2013) Role of Nrf2 in Oxidative Stress and Toxicity, *Annual Review of Pharmacology and Toxicology 53*, 401-426.

[34] Chan, K., Lu, R., Chang, J. C., and Kan, Y. W. (1996) NRF2, a member of the NFE2 family of transcription factors, is not essential for murine erythropoiesis, growth, and development, *Proceedings of the National Academy of Sciences of the United States of America 93*, 13943-13948.

[35] Sykiotis, G. P., and Bohmann, D. (2010) Stress-Activated Cap'n'collar Transcription Factors in Aging and Human Disease, *Science signaling 3*, re3-re3.

[36] Alam, J., Stewart, D., Touchard, C., Boinapally, S., Choi, A. M., and Cook, J. L. (1999) Nrf2, a Cap'n'Collar transcription factor, regulates induction of the heme oxygenase-1 gene, *The Journal of biological chemistry 274*, 26071-26078.

[37] Itoh, K., Mochizuki, M., Ishii, Y., Ishii, T., Shibata, T., Kawamoto, Y., Kelly, V., Sekizawa, K., Uchida, K., and Yamamoto, M. (2004) Transcription factor Nrf2 regulates inflammation by mediating the effect of 15-deoxy-Delta(12,14)-prostaglandin j(2), *Molecular and Cellular Biology 24*, 36-45.

[38] Brigelius-Flohe, R., and Flohe, L. (2011) Basic principles and emerging concepts in the redox control of transcription factors, *Antioxidants & redox signaling 15*, 2335-2381.

[39] Itoh, K., Wakabayashi, N., Katoh, Y., Ishii, T., Igarashi, K., Engel, J. D., and Yamamoto, M. (1999) Keap1 represses nuclear activation of antioxidant responsive elements by Nrf2 through binding to the amino-terminal Neh2 domain, *Genes & Development 13*, 76-86.

[40] Itoh, K., Ishii, T., Wakabayashi, N., and Yamamoto, M. (1999) Regulatory mechanisms of cellular response to oxidative stress, *Free Radical Research 31*, 319-324.

[41] Dhakshinamoorthy, S., and Jaiswal, A. K. (2001) Functional characterization and role of INrf2 in antioxidant response element-mediated expression and antioxidant induction of NAD(P)H:quinone oxidoreductase1 gene, *Oncogene 20*, 3906-3917.

[42] Kobayashi, A., Kang, M. I., Watai, Y., Tong, K. I., Shibata, T., Uchida, K., and Yamamoto, M. (2006) Oxidative and electrophilic stresses activate Nrf2 through inhibition of ubiquitination activity of Keap1, *Molecular and Cellular Biology 26*, 221-229.

[43] Zhang, D. D., and Hannink, M. (2003) Distinct cysteine residues in Keap1 are required for Keap1-dependent ubiquitination of Nrf2 and for stabilization of Nrf2 by chemopreventive agents and oxidative stress, *Molecular and Cellular Biology 23*, 8137-8151.

[44] Hilt, W., and Wolf, D. H. (1996) Proteasomes: destruction as a programme, *Trends in Biochemical Sciences 21*, 96-102.

[45] Nguyen, T., Sherratt, P. J., Huang, H. C., Yang, C. S., and Pickett, C. B. (2003) Increased protein stability as a mechanism that enhances Nrf2-mediated transcriptional activation of the antioxidant response element. Degradation of Nrf2 by the 26 S proteasome, *Journal of Biological Chemistry 278*, 4536-4541.

[46] Itoh, K., Wakabayashi, N., Katoh, Y., Ishii, T., O'Connor, T., and Yamamoto, M. (2003) Keap1 regulates both cytoplasmic-nuclear shuttling and degradation of Nrf2 in response to electrophiles, *Genes to Cells 8*, 379-391.

[47] Furukawa, M., and Xiong, Y. (2005) BTB protein Keap1 targets antioxidant transcription factor Nrf2 for ubiquitination by the Cullin 3-Roc1 ligase, *Molecular and Cellular Biology 25*, 162-171.

[48] Cullinan, S. B., Gordan, J. D., Jin, J., Harper, J. W., and Diehl, J. A. (2004) The Keap1-BTB protein is an adaptor that bridges Nrf2 to a Cul3-based E3 ligase: oxidative stress sensing by a Cul3-Keap1 ligase, *Molecular and Cellular Biology 24*, 8477-8486.

[49] Zhang, D. D., Lo, S. C., Cross, J. V., Templeton, D. J., and Hannink, M. (2004) Keap1 is a redox-regulated substrate adaptor protein for a Cul3-dependent ubiquitin ligase complex, *Molecular and Cellular Biology 24*, 10941-10953.

[50] Kobayashi, A., Kang, M. I., Okawa, H., Ohtsuji, M., Zenke, Y., Chiba, T., Igarashi, K., and Yamamoto, M. (2004) Oxidative stress sensor Keap1 functions as an adaptor for Cul3-based E3 ligase to regulate proteasomal degradation of Nrf2, *Molecular and Cellular Biology 24*, 7130-7139.

[51] Adams, J., Kelso, R., and Cooley, L. (2000) The kelch repeat superfamily of proteins: propellers of cell function, *Trends in Cell Biology 10*, 17-24.

[52] Itoh, K., Tong, K. I., and Yamamoto, M. (2004) Molecular mechanism activating nrf2–keap1 pathway in regulation of adaptive response to electrophiles, *Free Radical Biology and Medicine 36*, 1208-1213.

[53] Padmanabhan, B., Tong, K. I., Ohta, T., Nakamura, Y., Scharlock, M., Ohtsuji, M., Kang, M. I., Kobayashi, A., Yokoyama, S., and Yamamoto, M. (2006) Structural basis for defects of Keap1 activity provoked by its point mutations in lung cancer, *Molecular Cell 21*, 689-700.

[54] Zollman, S., Godt, D., Prive, G. G., Couderc, J. L., and Laski, F. A. (1994) The BTB domain, found primarily in zinc finger proteins, defines an evolutionarily conserved family that includes several developmentally regulated genes in Drosophila,

Proceedings of the National Academy of Sciences of the United States of America 91, 10717-10721.

[55] Watai, Y., Kobayashi, A., Nagase, H., Mizukami, M., McEvoy, J., Singer, J. D., Itoh, K., and Yamamoto, M. (2007) Subcellular localization and cytoplasmic complex status of endogenous Keap1, *Genes to Cells 12*, 1163-1178.

[56] Wakabayashi, N., Dinkova-Kostova, A. T., Holtzclaw, W. D., Kang, M. I., Kobayashi, A., Yamamoto, M., Kensler, T. W., and Talalay, P. (2004) Protection against electrophile and oxidant stress by induction of the phase 2 response: fate of cysteines of the Keap1 sensor modified by inducers, *Proceedings of the National Academy of Sciences of the United States of America 101*, 2040-2045.

[57] Zipper, L. M., and Mulcahy, R. T. (2002) The Keap1 BTB/POZ dimerization function is required to sequester Nrf2 in cytoplasm, *Journal of Biological Chemistry 277*, 36544-36552.

[58] Furukawa, M., He, Y. J., Borchers, C., and Xiong, Y. (2003) Targeting of protein ubiquitination by BTB-Cullin 3-Roc1 ubiquitin ligases, *Nature Cell Biology 5*, 1001-1007.

[59] Petroski, M. D., and Deshaies, R. J. (2005) Function and regulation of cullin-RING ubiquitin ligases, *Nature Reviews. Molecular Cell Biology 6*, 9-20.

[60] Dinkova-Kostova, A. T., Holtzclaw, W. D., Cole, R. N., Itoh, K., Wakabayashi, N., Katoh, Y., Yamamoto, M., and Talalay, P. (2002) Direct evidence that sulfhydryl groups of Keap1 are the sensors regulating induction of phase 2 enzymes that protect against carcinogens and oxidants, *Proceedings of the National Academy of Sciences of the United States of America 99*, 11908-11913.

[61] Itoh, K., Igarashi, K., Hayashi, N., Nishizawa, M., and Yamamoto, M. (1995) Cloning and characterization of a novel erythroid cell-derived CNC family transcription factor heterodimerizing with the small Maf family proteins, *Molecular and Cellular Biology 15*, 4184-4193.

[62] Rushmore, T. H., and Pickett, C. B. (1990) Transcriptional regulation of the rat glutathione S-transferase Ya subunit gene. Characterization of a xenobiotic-responsive element controlling inducible expression by phenolic antioxidants, *Journal of Biological Chemistry 265*, 14648-14653.

[63] Moinova, H. R., and Mulcahy, R. T. (1998) An electrophile responsive element (EpRE) regulates beta-naphthoflavone induction of the human gamma-glutamylcysteine synthetase regulatory subunit gene. Constitutive expression is mediated by an adjacent AP-1 site, *Journal of Biological Chemistry 273*, 14683-14689.

[64] Wakabayashi, N., Slocum, S. L., Skoko, J. J., Shin, S., and Kensler, T. W. (2010) When NRF2 talks, who's listening?, *Antioxidants and Redox Signaling 13*, 1649-1663.

[65] Zhu, M., and Fahl, W. E. (2001) Functional Characterization of Transcription Regulators That Interact with the Electrophile Response Element, *Biochemical and Biophysical Research Communications 289*, 212-219.

[66] Katoh, Y., Itoh, K., Yoshida, E., Miyagishi, M., Fukamizu, A., and Yamamoto, M. (2001) Two domains of Nrf2 cooperatively bind CBP, a CREB binding protein, and synergistically activate transcription, *Genes to Cells 6*, 857-868.

[67] Sun, Z., Chin, Y. E., and Zhang, D. D. (2009) Acetylation of Nrf2 by p300/CBP augments promoter-specific DNA binding of Nrf2 during the antioxidant response, *Molecular and Cellular Biology 29*, 2658-2672.

[68] Katsuoka, F., Motohashi, H., Ishii, T., Aburatani, H., Engel, J. D., and Yamamoto, M. (2005) Genetic evidence that small maf proteins are essential for the activation of antioxidant response element-dependent genes, *Molecular and Cellular Biology 25*, 8044-8051.

[69] Itoh, K., Chiba, T., Takahashi, S., Ishii, T., Igarashi, K., Katoh, Y., Oyake, T., Hayashi, N., Satoh, K., Hatayama, I., Yamamoto, M., and Nabeshima, Y.-i. (1997) An Nrf2/Small Maf Heterodimer Mediates the Induction of Phase II Detoxifying Enzyme

Genes through Antioxidant Response Elements, *Biochemical and Biophysical Research Communications 236*, 313-322.

[70] Zhu, H., Itoh, K., Yamamoto, M., Zweier, J. L., and Li, Y. (2005) Role of Nrf2 signaling in regulation of antioxidants and phase 2 enzymes in cardiac fibroblasts: protection against reactive oxygen and nitrogen species-induced cell injury, *FEBS Letters 579*, 3029-3036.

[71] Harvey, C. J., Thimmulappa, R. K., Singh, A., Blake, D. J., Ling, G., Wakabayashi, N., Fujii, J., Myers, A., and Biswal, S. (2009) Nrf2-regulated glutathione recycling independent of biosynthesis is critical for cell survival during oxidative stress, *Free Radical Biology and Medicine 46*, 443-453.

[72] Singh, A., Rangasamy, T., Thimmulappa, R. K., Lee, H., Osburn, W. O., Brigelius-Flohe, R., Kensler, T. W., Yamamoto, M., and Biswal, S. (2006) Glutathione peroxidase 2, the major cigarette smoke-inducible isoform of GPX in lungs, is regulated by Nrf2, *American Journal of Respiratory Cell and Molecular Biology 35*, 639-650.

[73] Akino, N., Wada-Hiraike, O., Terao, H., Honjoh, H., Isono, W., Fu, H., Hirano, M., Miyamoto, Y., Tanikawa, M., Harada, M., Hirata, T., Hirota, Y., Koga, K., Oda, K., Kawana, K., Fujii, T., and Osuga, Y. (2018) Activation of Nrf2 might reduce oxidative stress in human granulosa cells, *Molecular and Cellular Endocrinology 470*, 96-104.

[74] Shen, G., and Kong, A. N. (2009) Nrf2 plays an important role in coordinated regulation of Phase II drug metabolism enzymes and Phase III drug transporters, *Biopharmaceutics and Drug Disposition 30*, 345-355.

[75] Zhang, M., An, C., Gao, Y., Leak, R. K., Chen, J., and Zhang, F. (2013) Emerging roles of Nrf2 and phase II antioxidant enzymes in neuroprotection, *Progress in Neurobiology 100*, 30-47.

[76] Lee, J. M., Li, J., Johnson, D. A., Stein, T. D., Kraft, A. D., Calkins, M. J., Jakel, R. J., and Johnson, J. A. (2005) Nrf2, a multi-organ protector?, *FASEB Journal 19*, 1061-1066.

[77] Lee, J. M., Calkins, M. J., Chan, K., Kan, Y. W., and Johnson, J. A. (2003) Identification of the NF-E2-related factor-2-dependent genes conferring protection against oxidative stress in primary cortical astrocytes using oligonucleotide microarray analysis, *Journal of Biological Chemistry 278*, 12029-12038.

[78] Sand, O., Sjaastad, Ø. V., Haug, E., Bjålie, J. G., and Toverud, K. C. (2006) *Menneskekroppen : fysiologi og anatomi*, 2. ed., Gyldendal akademisk, Oslo.

[79] Bain, B. J. (2017) Structure and function of red and white blood cells, *Medicine 45*, 187-193.

[80] Gordon-Smith, T. (2013) Structure and function of red and white blood cells, *Medicine 41*, 193-199.

[81] Ashton, N. (2013) Physiology of red and white blood cells, *Anaesthesia & Intensive Care Medicine 14*, 261-266.

[82] Kleiveland, C. R. (2015) Peripheral Blood Mononuclear Cells, In *The Impact of Food Bioactives on Health: in vitro and ex vivo models* (Verhoeckx, K., Cotter, P., López-Expósito, I., Kleiveland, C., Lea, T., Mackie, A., Requena, T., Swiatecka, D., and Wichers, H., Eds.), pp 161-167, Springer International Publishing, Cham.

[83] Rodak, B. F., Fritsma, G. A., and Doig, K. (2007) *Hematology : clinical principles and applications*, 3. ed., Saunders Elsevier, St. Louis, Mo.

[84] Cavenagh, J. (2007) White blood cells, *Surgery (Oxford) 25*, 61-64.

[85] Damjanov, I. (2012) *Pathology for the health professions*, 4. ed., Elsevier Saunders, St. Louis, Missouri.

[86] Kobayashi, E., Suzuki, T., and Yamamoto, M. (2013) Roles nrf2 plays in myeloid cells and related disorders, *Oxidative Medicine and Cellular Longevity 2013*, 529219.

[87] Mahmood, T., and Yang, P.-C. (2012) Western Blot: Technique, Theory, and Trouble Shooting, *North American Journal of Medical Sciences 4*, 429-434.

[88] Walker, J. M., and Wilson, K. (2010) *Principles and techniques of biochemistry and molecular biology*, 7th ed. ed., Cambridge University Press, Cambridge.

[89] Smejkal, G. B., Shainoff, J. R., and Kottke-Marchant, K. M. (2003) Rapid high-resolution electrophoresis of multimeric von Willebrand Factor using a thermopiloted gel apparatus, *Electrophoresis 24*, 582-587.

[90] Bass, J. J., Wilkinson, D. J., Rankin, D., Phillips, B. E., Szewczyk, N. J., Smith, K., and Atherton, P. J. (2017) An overview of technical considerations for Western blotting applications to physiological research, *Scandinavian Journal of Medicine & Science in Sports 27*, 4-25.

[91] Rehm, H. (2006) *Protein biochemistry and proteomics*, 4. ed., Academic Press, Burlington, Mass.

[92] Chang, R. (2005) *Physical chemistry : for the biosciences*, University Science Books, Sausalito, California.

[93] Active Motif, Inc. (2014) TransAM®Nrf2 (version A3), Active Motif.

[94] Nabbi, A., and Riabowol, K. (2015) Rapid Isolation of Nuclei from Cells In Vitro, *Cold Spring Harb Protoc 2015*, 769-772.

[95] Goldman, A., Harper, S., and Speicher, D. W. (2016) Detection of Proteins on Blot Membranes, *Current protocols in protein science 86*, 10.18.11-10.18.11.

[96] Linnet, K., and Kondratovich, M. (2004) Partly nonparametric approach for determining the limit of detection, *Clinical Chemistry 50*, 732-740.

[97] Schneider, C. A., Rasband, W. S., and Eliceiri, K. W. (2012) NIH Image to ImageJ: 25 years of image analysis, *Nature Methods 9*, 671-675.

[98] Murakami, S., Shimizu, R., Romeo, P. H., Yamamoto, M., and Motohashi, H. (2014) Keap1-Nrf2 system regulates cell fate determination of hematopoietic stem cells, *Genes to Cells 19*, 239-253.

[99] Lau, A., Tian, W., Whitman, S. A., and Zhang, D. D. (2013) The Predicted Molecular Weight of Nrf2: It Is What It Is Not, *Antioxidants & Redox Signaling 18*, 91-93.

[100] The UniProt Consortium. (2017) UniProt: the universal protein knowledgebase, *Nucleic Acids Research 45*, D158-D169.

[101] Guan, Y., Zhu, Q., Huang, D., Zhao, S., Jan Lo, L., and Peng, J. (2015) An equation to estimate the difference between theoretically predicted and SDS PAGE-displayed molecular weights for an acidic peptide, *Scientific Reports 5*, 13370.

[102] Li, Y., Paonessa, J. D., and Zhang, Y. (2012) Mechanism of chemical activation of Nrf2, *PloS One 7*, e35122.

[103] Pi, J., Bai, Y., Reece, J. M., Williams, J., Liu, D., Freeman, M. L., Fahl, W. E., Shugar, D., Liu, J., Qu, W., Collins, S., and Waalkes, M. P. (2007) Molecular mechanism of human Nrf2 activation and degradation: role of sequential phosphorylation by protein kinase CK2, *Free Radical Biology and Medicine 42*, 1797-1806.

[104] Apopa, P. L., He, X., and Ma, Q. (2008) Phosphorylation of Nrf2 in the transcription activation domain by casein kinase 2 (CK2) is critical for the nuclear translocation and transcription activation function of Nrf2 in IMR-32 neuroblastoma cells, *Journal of Biochemical and Molecular Toxicology 22*, 63-76.

[105] Kemmerer, Z. A., Ader, N. R., Mulroy, S. S., and Eggler, A. L. (2015) Comparison of human Nrf2 antibodies: A tale of two proteins, *Toxicology Letters 238*, 83-89.

[106] Hornbeck, P. V., Zhang, B., Murray, B., Kornhauser, J. M., Latham, V., and Skrzypek, E. (2015) PhosphoSitePlus, 2014: mutations, PTMs and recalibrations, *Nucleic Acids Research 43*, D512-D520.

[107] Ohtsubo, T., Kamada, S., Mikami, T., Murakami, H., and Tsujimoto, Y. (1999) Identification of NRF2, a member of the NF-E2 family of transcription factors, as a substrate for caspase-3(-like) proteases, *Cell Death and Differentiation 6*, 865-872.

[108] Malloy, M. T., McIntosh, D. J., Walters, T. S., Flores, A., Goodwin, J. S., and Arinze, I. J. (2013) Trafficking of the transcription factor Nrf2 to promyelocytic leukemia-nuclear bodies: implications for degradation of NRF2 in the nucleus, *Journal of Biological Chemistry 288*, 14569-14583.

[109] Nguyen, T., Sherratt, P. J., Nioi, P., Yang, C. S., and Pickett, C. B. (2005) Nrf2 controls constitutive and inducible expression of ARE-driven genes through a dynamic pathway involving nucleocytoplasmic shuttling by Keap1, *Journal of Biological Chemistry 280*, 32485-32492.

[110] Urban, P. L. (2016) Quantitative mass spectrometry: an overview, *Philosophical transactions. Series A, Mathematical, physical, and engineering sciences 374*, 20150382.

Appendix 1: Samples and their labelling

An overview of lysates and their labelling is presented in table 1. Fractions and their labelling used in purity determination and detection of Nrf2 are presented table 2.

Table 1. Overview of lysates used in evaluation of isolation of PBMCs and characterization of Nrf2.

Person	Number of blood samples	Labelling	Test material	Experiment
P1	6	1-1	Lysate	Method 1-Evaluation of isolation of PBMCs
		1-2		
		1-3		
		1-4	Lysate	Method 2-Evaluation of isolation of PBMCs
		1-5		
		1-6		
P2	6	2-1	Lysate	Method 1-Evaluation of isolation of PBMCs
		2-2		
		2-3		
		2-4	Lysate	Method 2-Evaluation of isolation of PBMCs
		2-5		
		2-6		
P3	6	3-1	Lysate	Method 1-Evaluation of isolation of PBMCs
		3-2		
		3-3		
		3-4	Lysate	Method 2-Evaluation of isolation of PBMCs
		3-5		
		3-6		
P4	3	L1	Lysate	WB-Characterization of Nrf2
P5	3	L2	Lysate	WB-Characterization of Nrf2
P6	3	L3	Lysate	WB-Characterization of Nrf2

Table 2. List over fractions used in purity determination and detection of Nrf2. "a": nuclear fraction obtained from fractionation of isolated cells from two of the three CPTs, while "b": nuclear fraction obtained from fractionation of isolated cells from one of the three CPTs.

Person	Number of blood samples	Labelling	Test material	Experiment
F4	2	W4	Whole cell fraction	Chemiluminescent WB-Nrf2 detection and purity determination
		C4	Cytosolic fraction	
		N4	Nuclear fraction	
F5	2	W5	Whole cell fraction	
		C5	Cytosolic fraction	
		N5	Nuclear fraction	
F6	2	W6	Whole cell fraction	
		C6	Cytosolic fraction	
		N6	Nuclear fraction	
F7	2	N7	Whole cell fraction	
		C7	Cytosolic fraction	
		N7	Nuclear fraction	
F8	2	W8	Whole cell fraction	Fluorescent WB-Nrf2 detection and purity determination
		C8	Cytosolic fraction	
		N8	Nuclear fraction	
F9	2	W9	Whole cell fraction	
		C9	Cytosolic fraction	
		N9	Nuclear fraction	
F10	2	W10	Whole cell fraction	
		C10	Cytosolic fraction	
		N10	Nuclear fraction	
F11	2	W11	Whole cell fraction	
		C11	Cytosolic fraction	
		N11	Nuclear fraction	
F12	3	N12a	Nuclear fraction	ELISA-based TransAM Nrf2 detection
		N12b	Nuclear fraction	
F13	3	N13a	Nuclear fraction	
		N13b	Nuclear fraction	
F14	3	N14a	Nuclear fraction	
		N14b	Nuclear fraction	
F15	3	N15a	Nuclear fraction	
		N15b	Nuclear fraction	
F16	2	C16	Cytosolic fraction	
		N16	Nuclear fraction	
F17	2	C17	Cytosolic fraction	
		N17	Nuclear fraction	
F18	2	C18	Cytosolic fraction	
		N18	Nuclear fraction	
F19	2	C19	Cytosolic fraction	
		N19	Nuclear fraction	

Appendix 2: Solutions

10% sodium deoxycholate stock solution:

For 10 mL:

1 g sodium deoxycholate

9 g (9 mL) ultrapure water

1% sodium dodecyl sulphate (SDS) stock solution:

For 10 mL:

0,1 g SDS

9,9 mL ultrapure water

Radioimmunoprecipitation assay (RIPA) buffer:

	For 500 mL:
150 mM sodium chloride	4.38 g
1.0% NP-40 10% (w/v)	5 mL
0.5% sodium deoxycholate	2.5 mL of a 10 % stock solution
0.1% SDS	0.5 mL of a 1% stock solution
50 mM Tris, pH 8.0	3.03 g

1. Dissolve 3.03 g Tris in 300 mL of ultrapure water
2. Adjust pH to 8.0 with HCl fuming 37%
3. Add the rest of the chemicals
4. Add ultrapure water to bring the volume to 500 mL

Phosphate-buffered saline (1x *PBS)*

1 PBS pack (0.1 M sodium phosphate, 0.15 M sodium chloride, pH 7.2)

Dissolve in a final volume of 500 mL of ultrapure water

0.1% NP-40 in ice-cold PBS 1x

For 100 mL:

1 mL NP-40 10% (w/v)

99 mL PBS 1x

Tris-buffered saline 20x *(*20x *TBS)*

For 500 mL:

24 g Tris

88 g NaCl

1. Dissolve in 350 mL of ultrapure water
2. Adjust pH to 7.6 with HCl fuming 37%
3. Add ultrapure water to bring the volume to 500 mL

Tris-buffered saline 1x *(*1x *TBS)*

For 500 mL:

25 mL TBS 20x

475 mL of ultrapure water

1x *Tris-buffer saline with 0.1 % Tween® 20 (TBST)*

For 500 mL:

25 mL TBS 20x

475 mL of ultrapure water

500 µL Tween® 20

Blocking buffer (TBST with 5% (w/v) milk or BSA)

For 15 mL:

0.75 g milk or BSA

Dissolve in a final volume of 15 mL TBST

TBST with 3% (w/v) milk or BSA

For 15 mL:

0.45 g milk or BSA

Dissolve in a final volume of 15 mL TBST

Stripping buffer

	For 1 L:
200 mM glycine, pH 2.2	15 g glycine
0.1 % (w/v) SDS	1 g SDS
1 % (v/v) Tween® 20	10 mL Tween® 20

1. Dissolve in 800 mL ultrapure water
2. Adjust pH to 2.2 with HCl fuming 37%
3. Add ultrapure water to bring the volume to 1 L

1x *Azure fluorescent blot washing solution*

For 300 mL:

30 mL of 10x Azure fluorescent blot wash buffer (provided in the purchased kit)

270 mL of ultrapure water

Appendix 3: Supersignal molecular weight protein ladder

Figure 1 shows supersignal molecular weight protein ladder. The protein ladder was diluted at 1:50 in 4x LDS and ultrapure water before it was used in Western blot to estimate the molecular weights (MWs) of proteins detected.

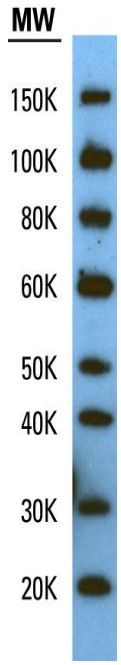

Figure 1: Supersignal molecular weight protein ladder (Thermo Fisher Scientific) on a NuPAGE® Novex® 4-12% Bis-Tris gel.

Appendix 4: Bradford assay-Representative calibration standard curve

The absorbance at 595 nm of the standards (table 3.3, page 27) was read in Synergy H1 microplate reader. The linear regression line was plotted as the dashed line in figure 2.

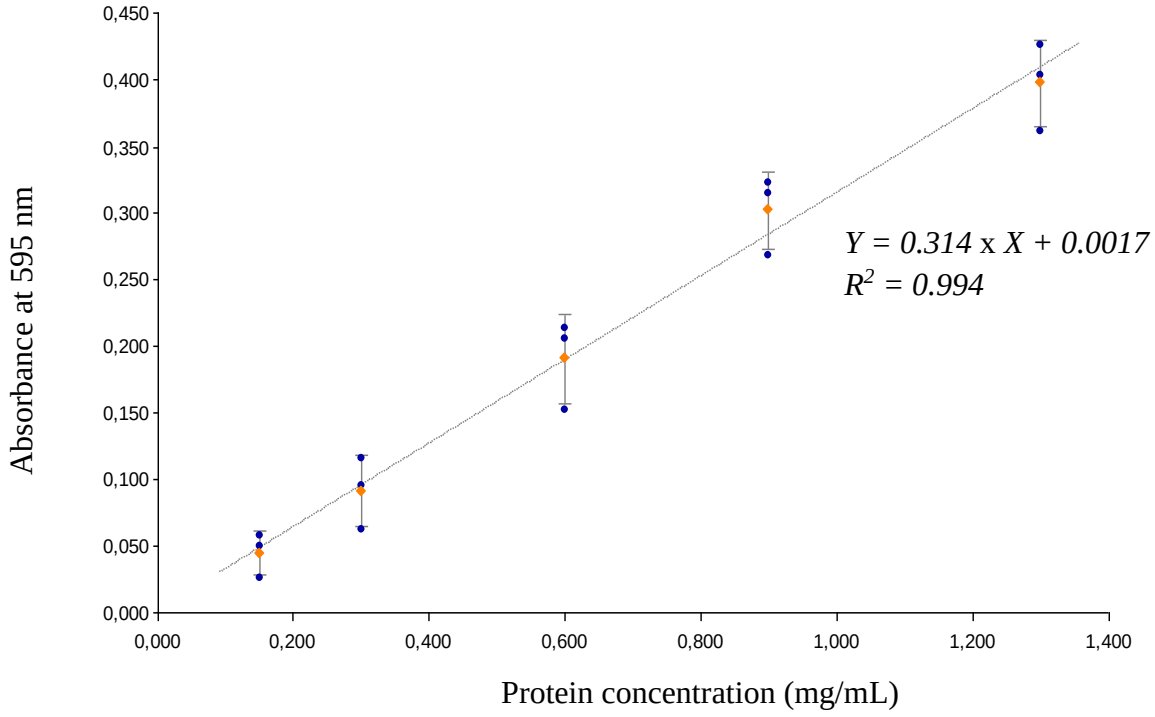

Figure 2. Representative BSA calibration standard curve used in Bradford assay for total protein determination. Orange points represents the average protein concentrations of each set of triplicate standards. Each error bar represents the average ± SD. Y: Absorbance at wavelength of 595 nm. X (mg/mL): protein concentration. R^2: coefficient of determination.